



JAMS

Damage Tolerance and Durability of Fiber-Metal Laminates for Aircraft Structures

Professor Jenn-Ming Yang



UCLA



The Joint Advanced Materials and Structures Center of Excellence

Damage Tolerance and Durability of Fiber-Metal Laminates for Aircraft Structures

- **Motivation and Key Issues**
 - **Fiber metal laminate is a new generation of primary structure for pressurized transport fuselage. However, there are limited and insufficient information available about mechanical behavior of FML in the published literature, and some areas still remains to be further verified by more detailed testing and analysis.**
- **Objective**
 - **To investigate the damage tolerance and durability of bi-directionally reinforced GLARE laminates. Such information will be used to support the airworthiness certification of GLARE structures**
- **Approach**
 - **To develop analytical methods validated by experiments**
 - **To develop information system**

FAA Sponsored Project Information

- **Principal Investigators & Researchers**

Hyoungeock Seo, PhD student

Pouy Chang, PhD student

Professor H. Thomas Hahn

Professor Jenn-Ming Yang

Department of Mechanical & Aerospace Engineering

Department Materials Science Engineering

University of California, Los Angeles

- **FAA Technical Monitor**

- **Mr. Curtis Davies**

- **Other FAA Personnel Involved**

-

- **Industry Participation**

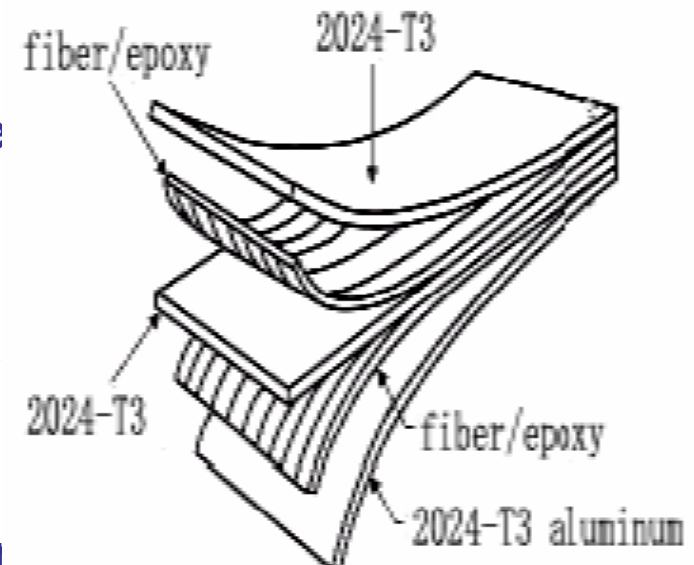
-

□ GLARE (GLAss fiber REinforced aluminum) laminates

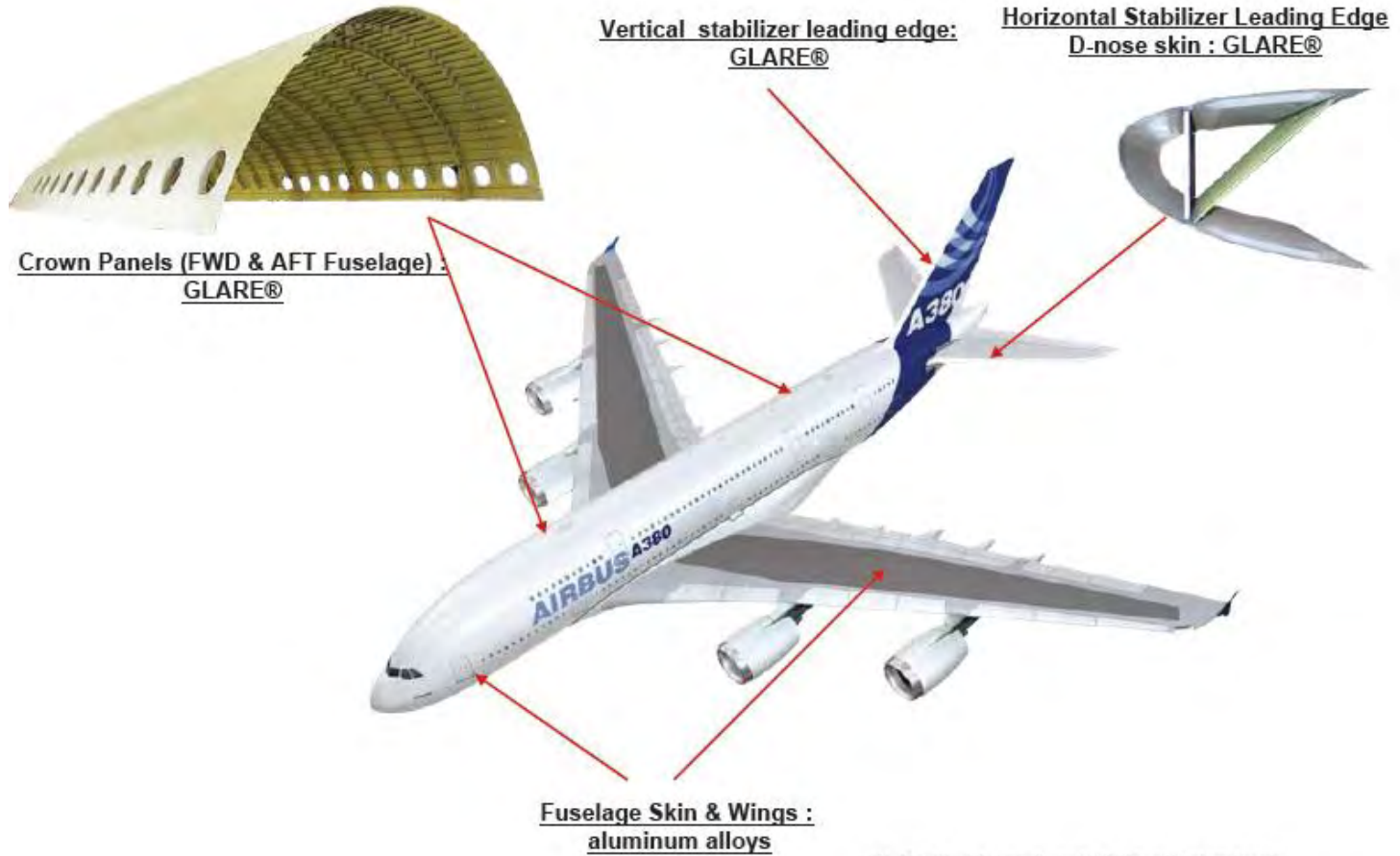
- Hybrid composites consisting of alternating thin metal layers and glass fibers

□ Advantages of GLARE

- High specific static mechanical properties and low density
- Outstanding fatigue resistance
- Excellent impact resistance and damage tolerance
- Good corrosion and durability
- Easy inspection like aluminum structures
- Excellent flame resistance



Applications of GLARE in A380



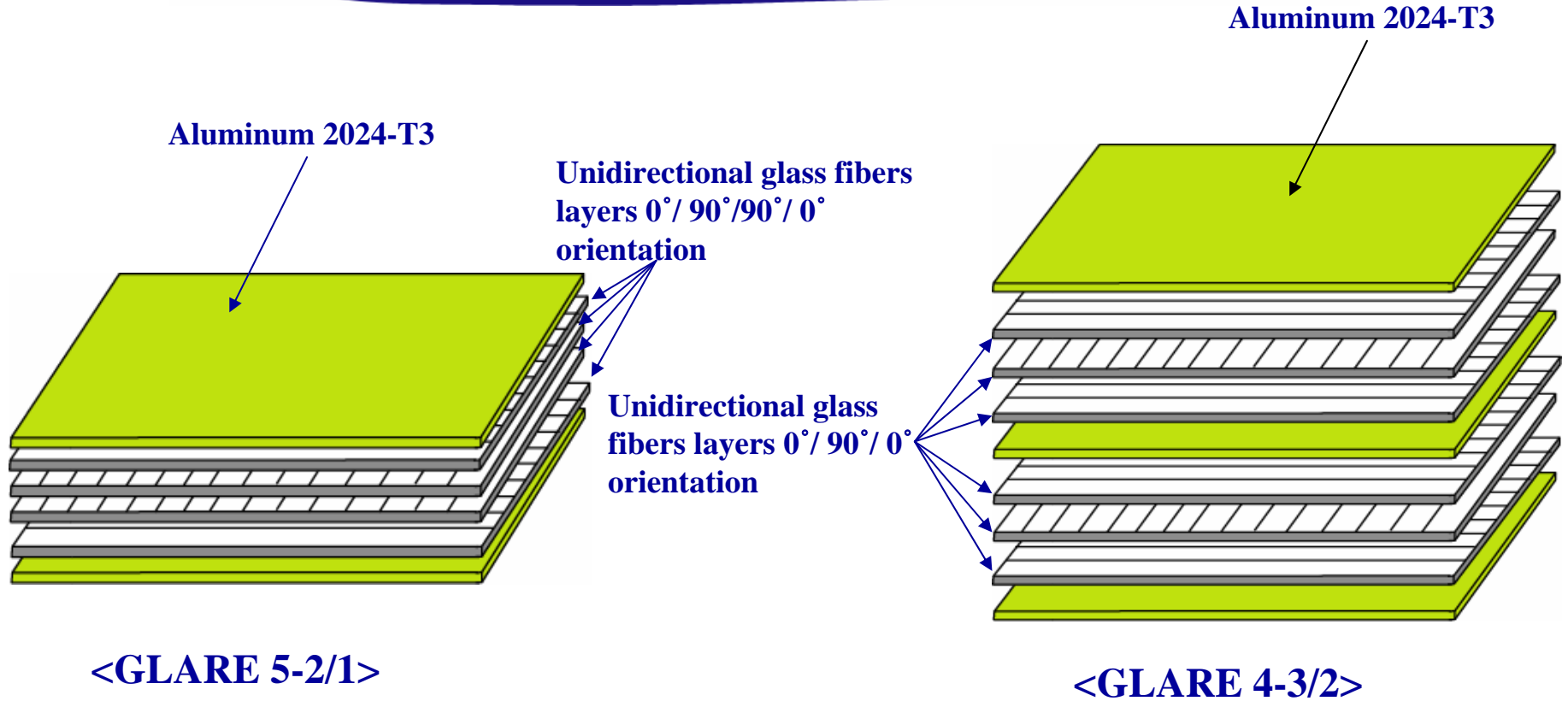
GLARE®: GLAss fiber REinforced aluminum

Background/GLARE laminates

Grade	Al layers		Fiber layers		Typical density (g/cm ³)
	Alloy	Thickness per layer (mm)	Orientation	Thicknesses per layer (mm)	
GLARE 1	7475-T6	0.3-0.4	Unidirectional	0.25	2.52
GLARE 2	2024-T3	0.2-0.5	Unidirectional	0.25	2.52
GLARE 3	2024-T3	0.2-0.5	0°/90° Cross-ply (50%-50%)	0.25	2.52
GLARE 4	2024-T3	0.2-0.5	0°/90°/0° Cross-ply (67%-33%)	0.375	2.45
GLARE 5	2024-T3	0.2-0.5	0°/90°/90°/0° Cross-ply (50%-50%)	0.5	2.38
GLARE 6	2024-T3	0.2-0.5	+45° /-45° Cross-ply (50%-50%)	0.25	2.52

To develop methodologies for guiding material development, property optimization and airworthiness certification:

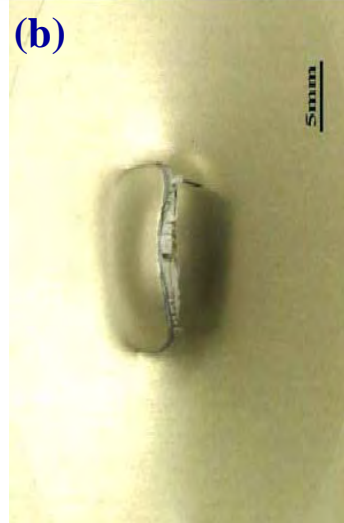
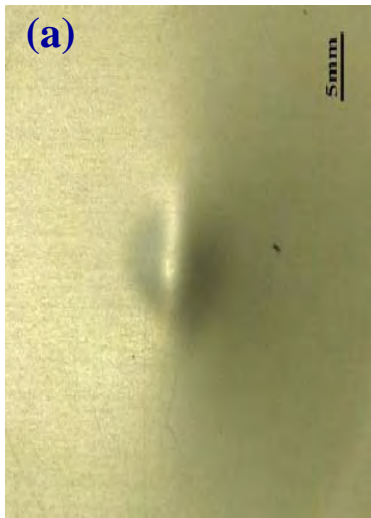
- **Residual Strength Modeling and Validation**
 - open-hole notch strength
 - residual strength after impact
 - open-hole notch strength after fatigue
- **Post-Impact Fatigue Behavior**
- **Fatigue Crack Growth Modeling and Validation**



* Provided by Aviation Equipment, Inc. (Costa, Mesa, CA)

Impact and Post-Impact Fatigue

- **Impact behavior**
 - Apply three different levels of impact energy to inflict different damages such as barely visible (dent), clearly visible (crack) and perforation
 - Characterize the extent of impact damage & strength retention
- **Post-impact fatigue behavior**
 - Measure the fatigue crack initiation life
 - Measure the crack length vs fatigue cycles
 - S-N curves
 - Investigation of crack propagation at inner and outer metal layer by NDT (x-ray and ultrasonic c-scan method)

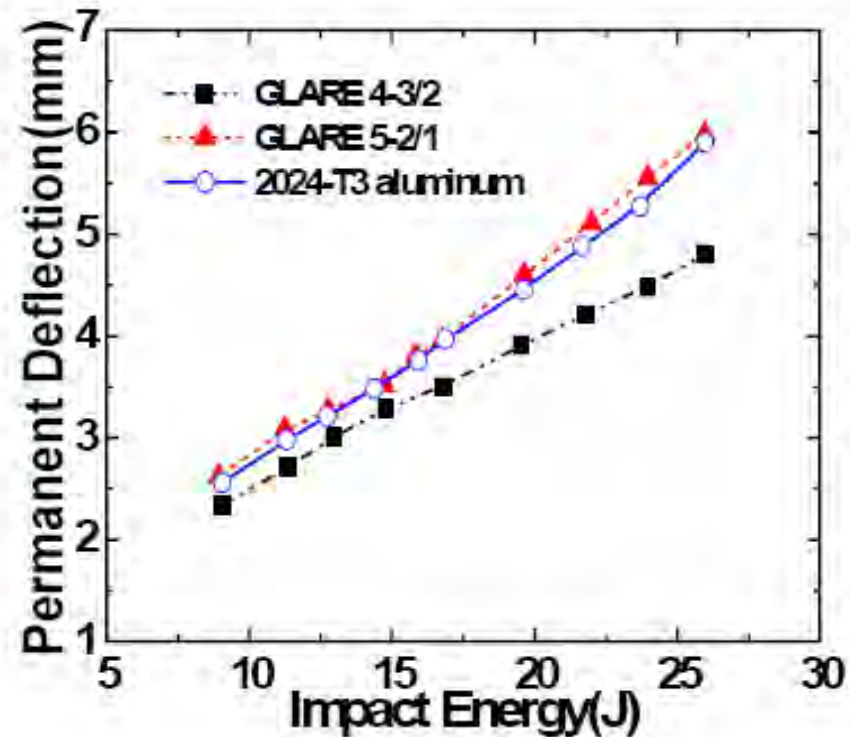
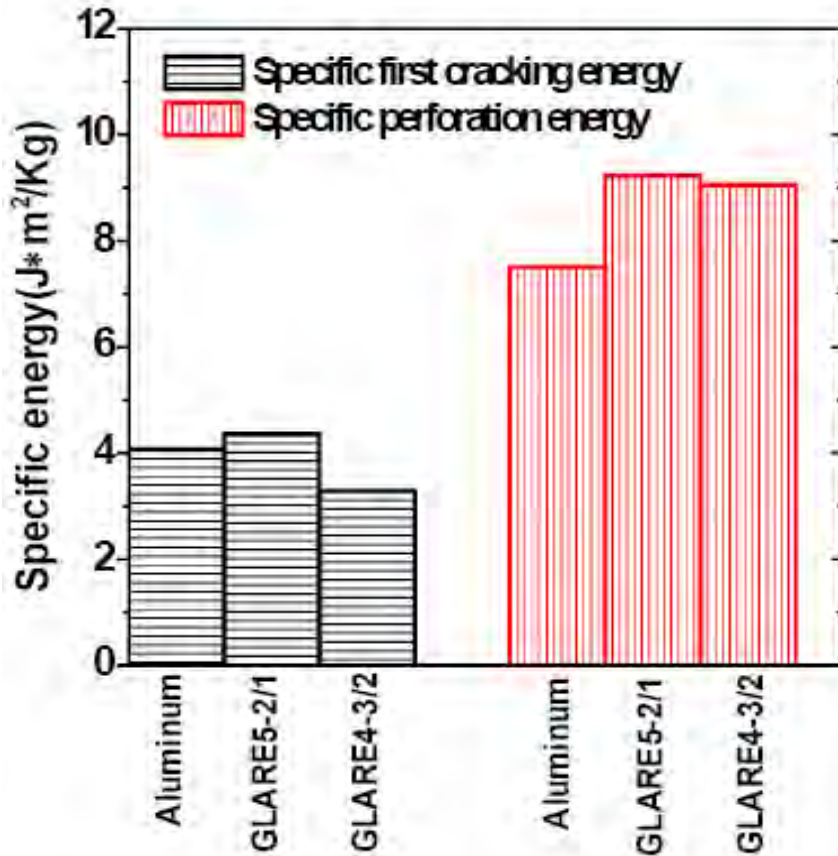


(a) Dent damage
 (E=10.8 J)
 GLARE 5

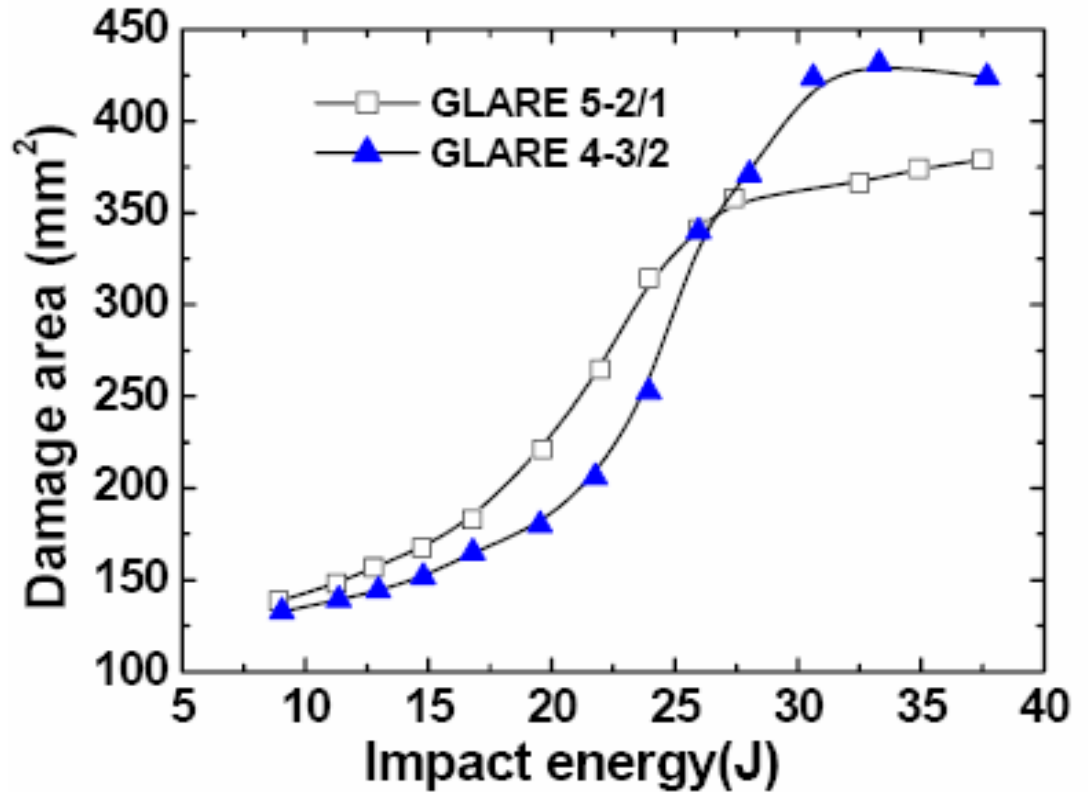
(b) Crack damage
 (E=18.1 J)
 GLARE 5

(c) Dent damage
 (E=10.8 J)
 GLARE 4

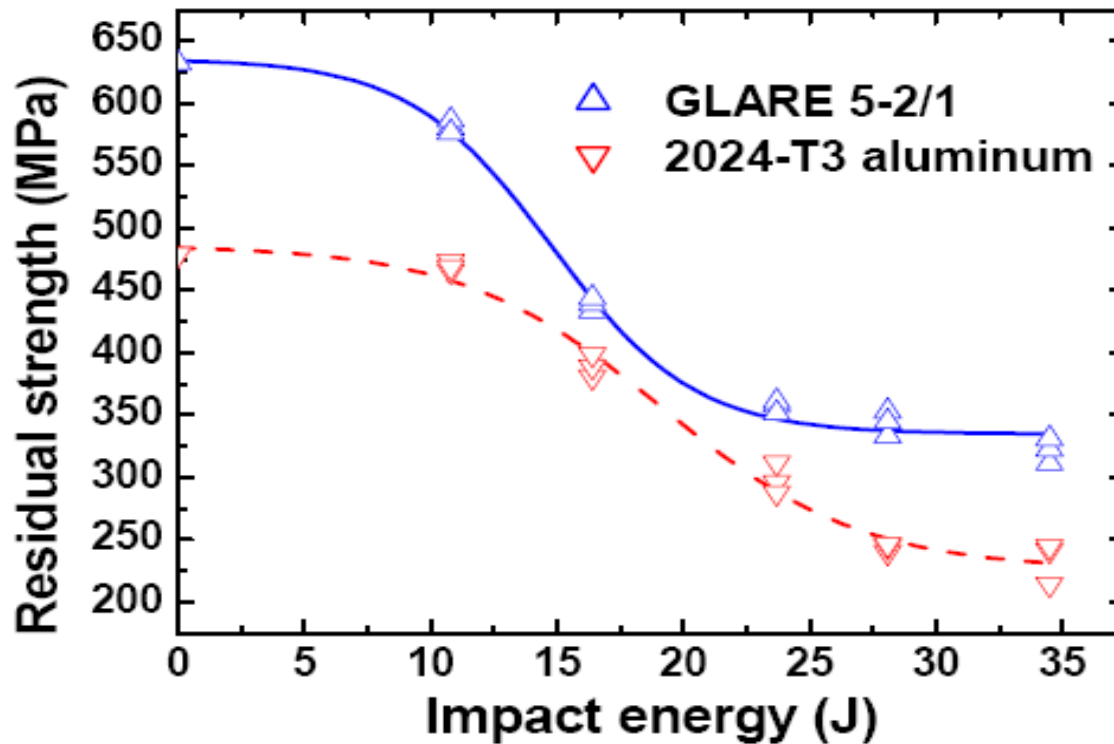
(d) Crack damage
 (E=18.1 J)
 GLARE 4



* Guocai Wu, et.al., Journal of material science (in press)



* Guocai Wu, et.al., Journal of material science (in press)



<Residual strength after impact at different energy levels>

* Guocai Wu, et.al., Journal of material science (in press)

- Post-impact fatigue test
 - Load ratio $R=0.1$
 - Cyclic loading
 - Impact energy: 10.8, 18.1 and 34.5 J
 - Load level: 20, 30, 40, 50 and 60% of residual strength
 - Frequency: 10 Hz



Crack growth for GLARE 4 with visible impact damage



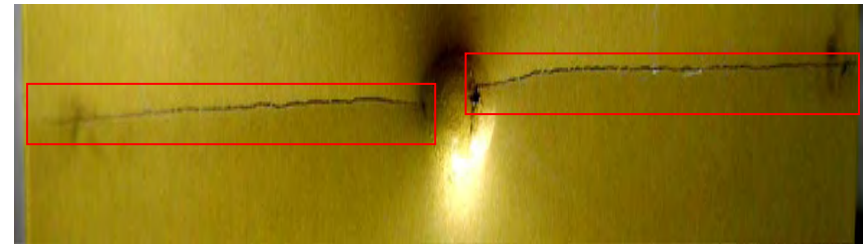
N=0 cycle



N=292584 cycle



N=472584 cycle



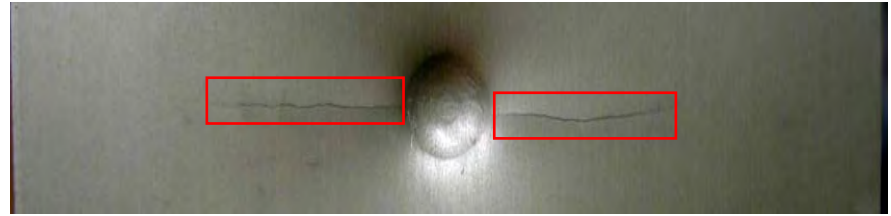
N=1002590 cycle

Crack initiated at the impacted side

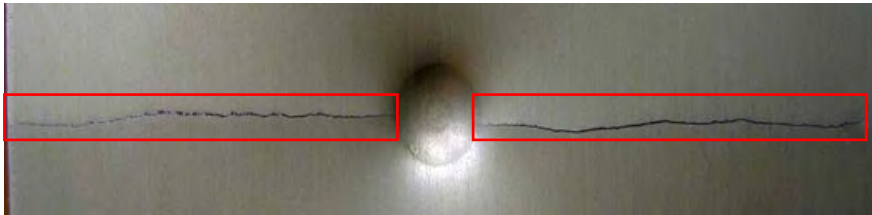
Crack growth for GLARE 5 with visible impact damage



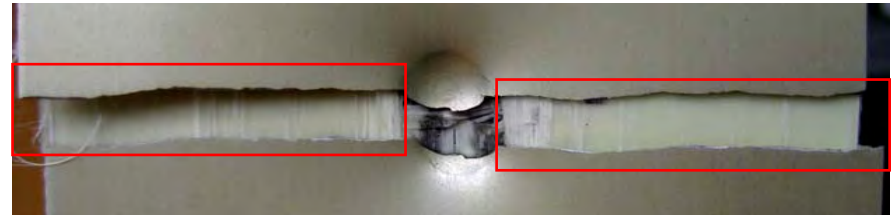
N=0 cycle



N=115000 cycle



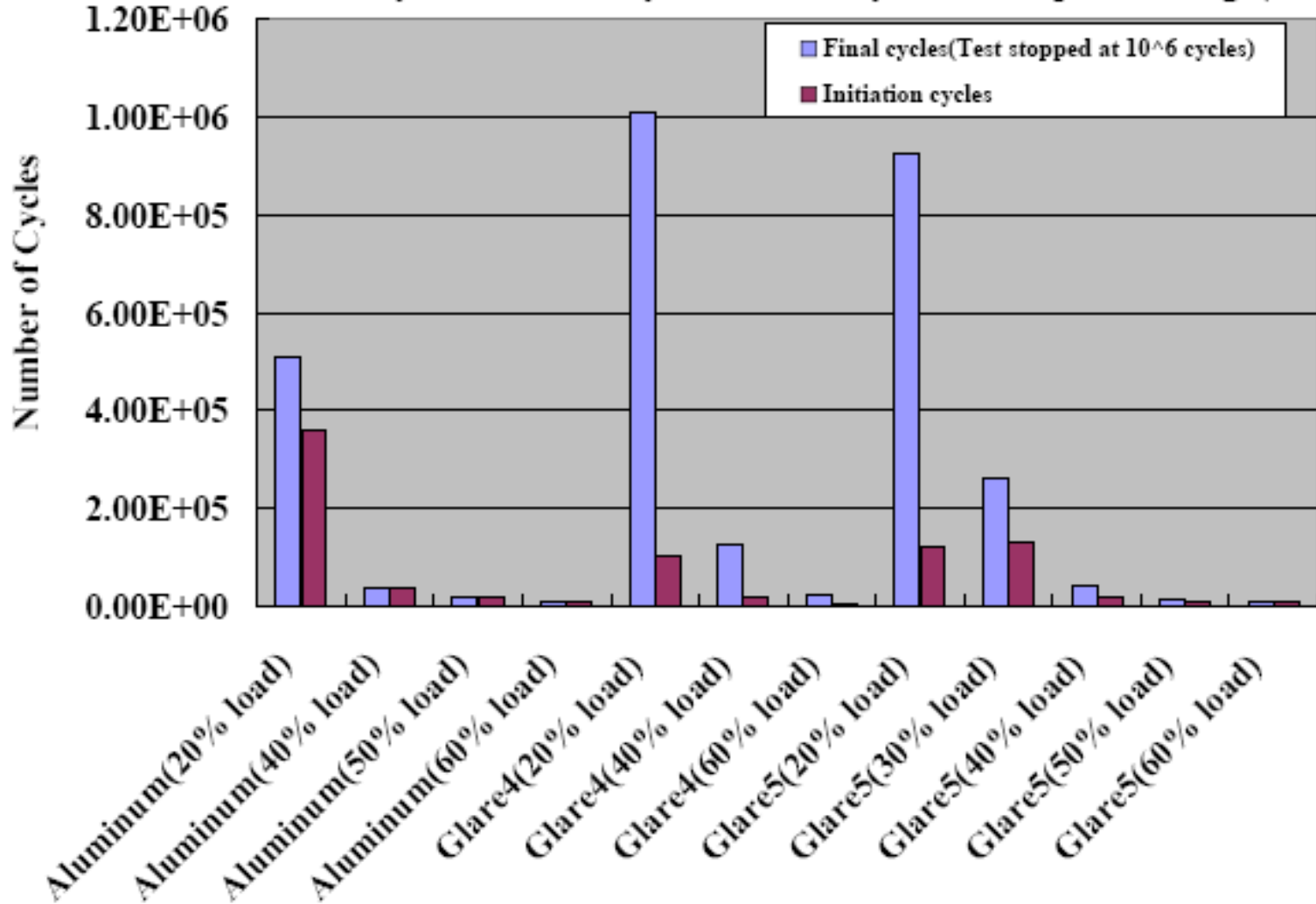
N=180000 cycle



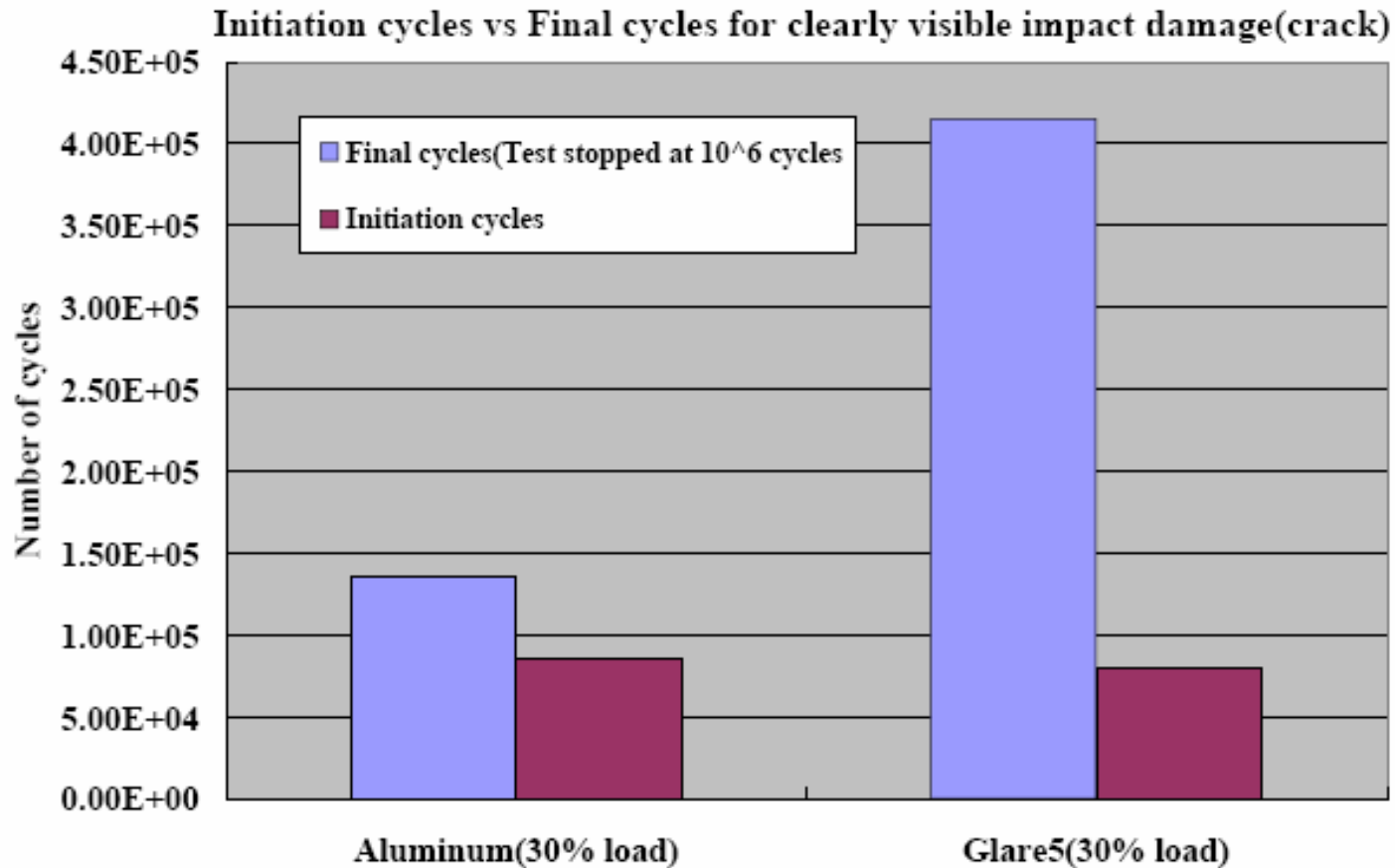
N=433541 cycle

Fatigue crack initiation vs. final cycle

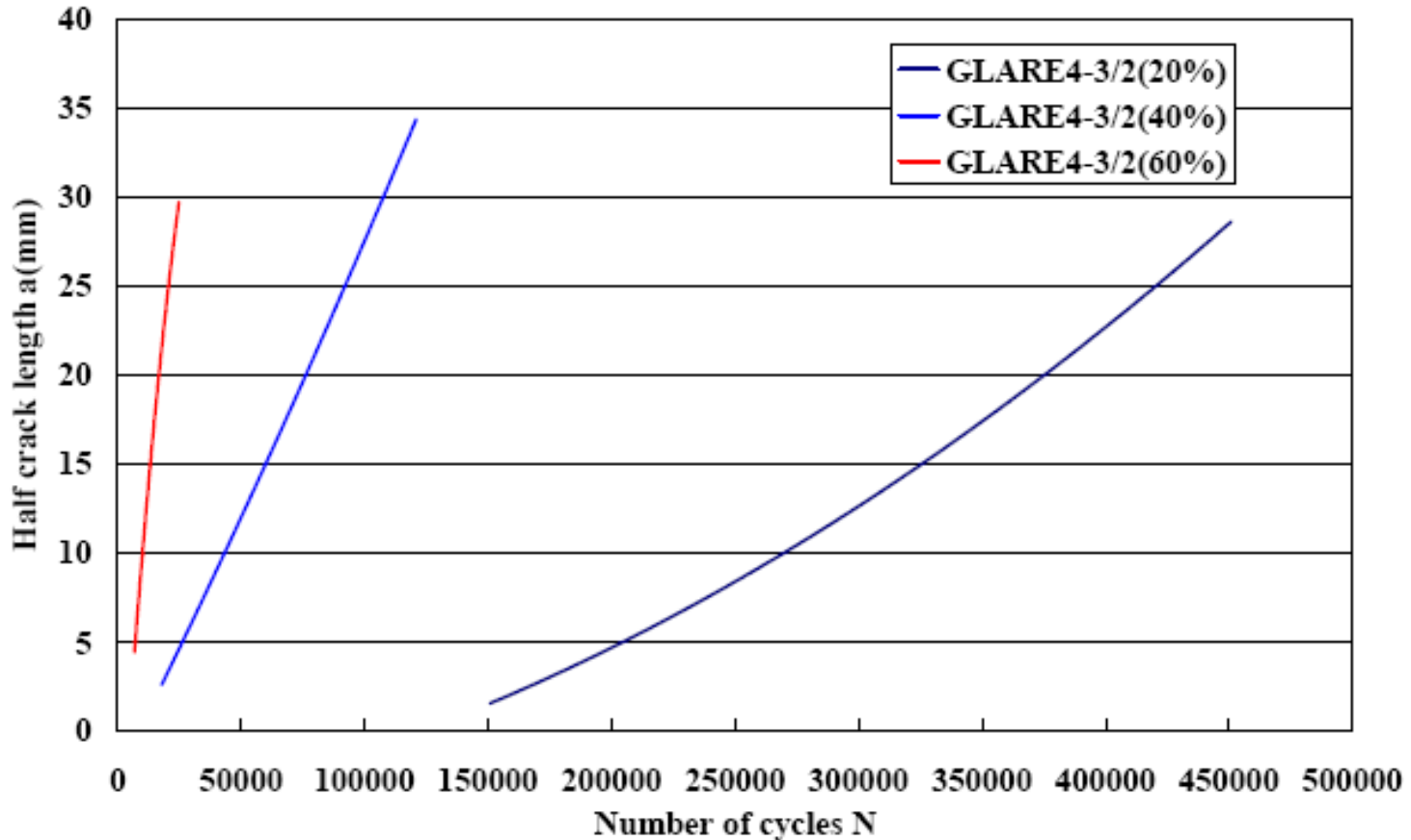
Initiation cycles vs. Final cycles for barely visible impact damage(dent)



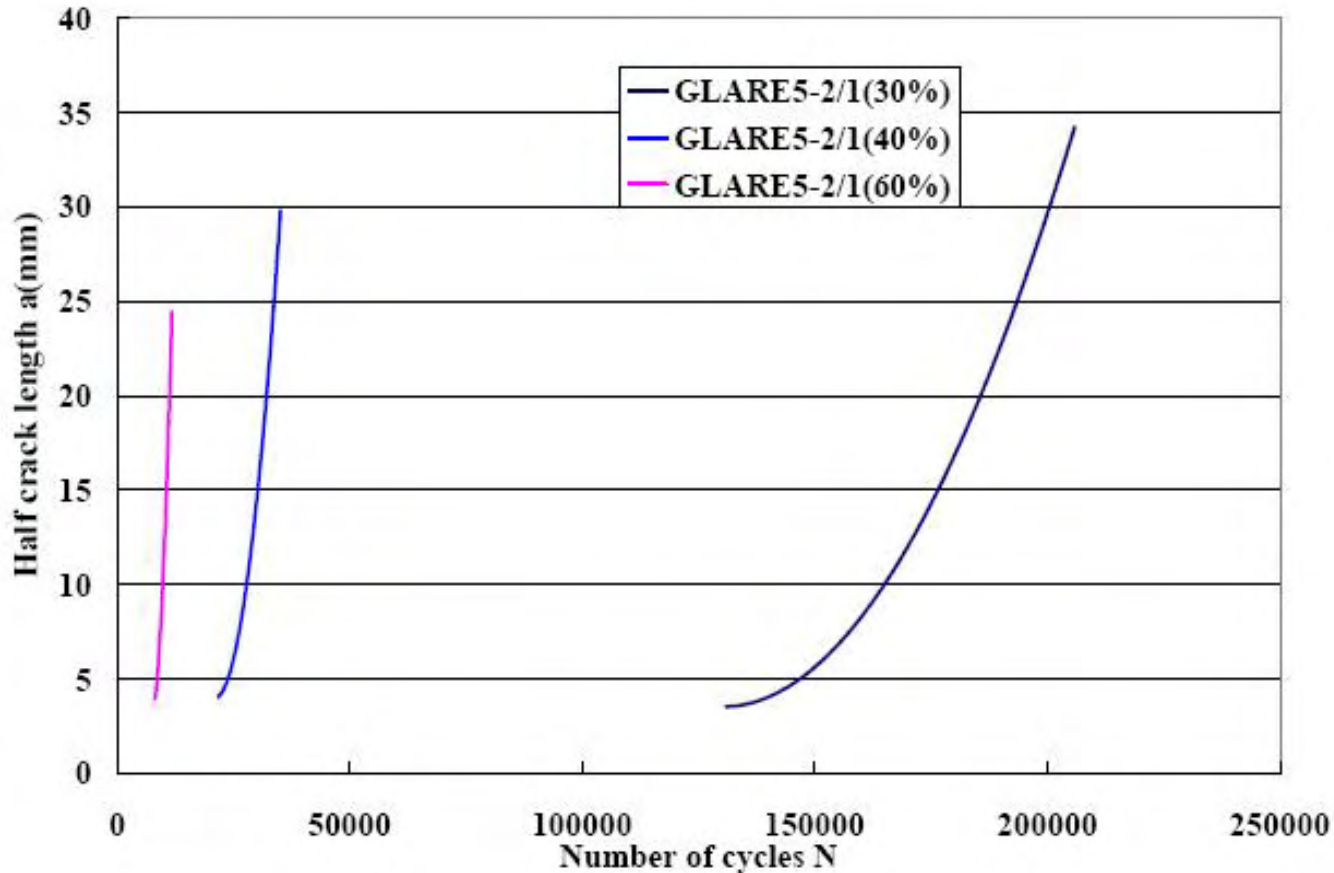
Post-Impact Fatigue Life for Visible Impact Damage (crack)



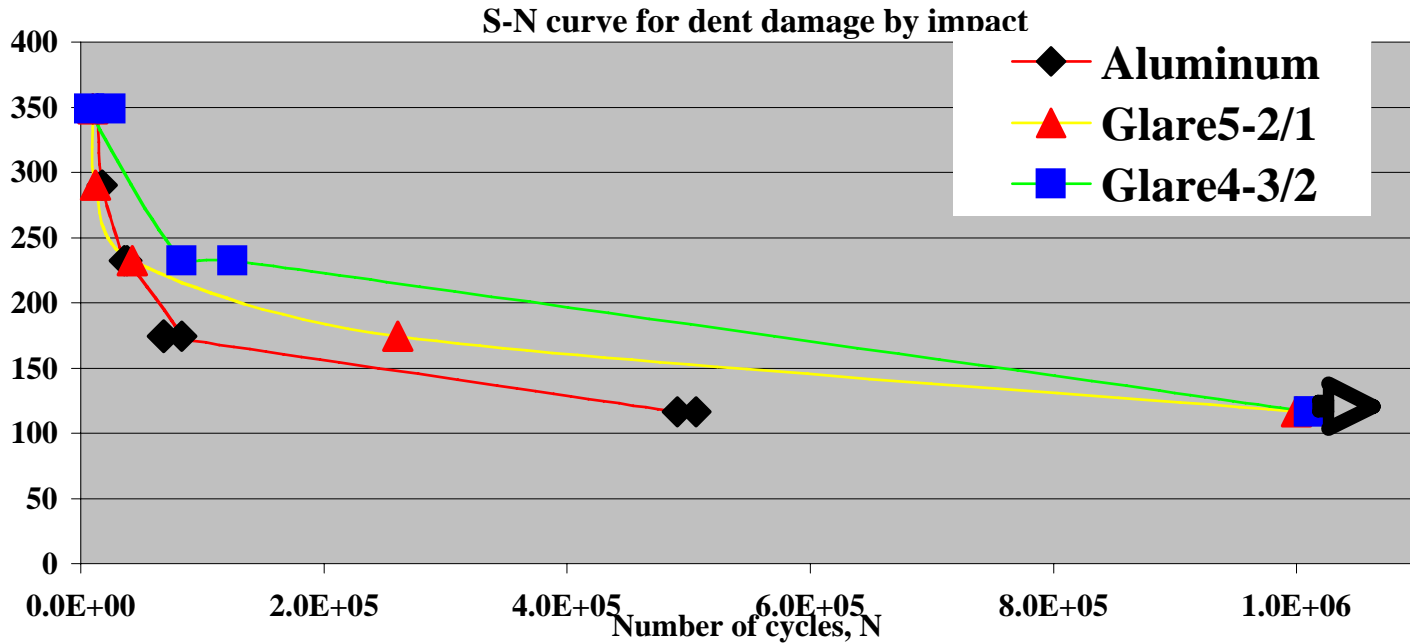
Fatigue Crack Growth with an Impacted Dent (GLARE4)



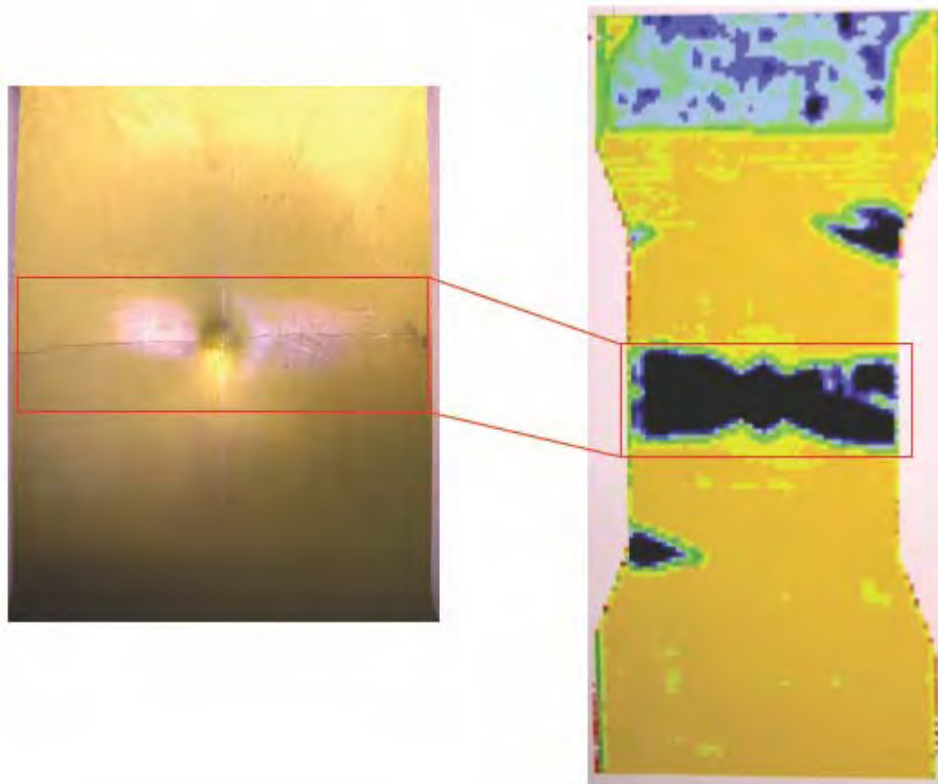
Fatigue Crack Growth with an Impacted Dent (GLARE5)



S-N curve for GLARE for barely visible impact damage

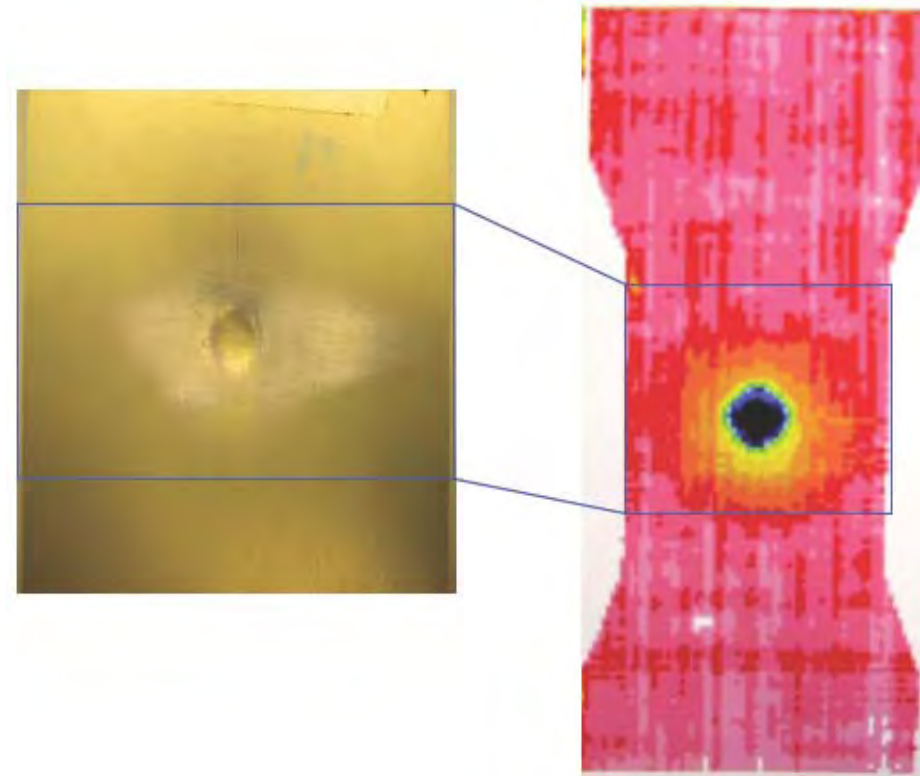


Ultrasonic c-scan images for GLARE



Glare 4-3/2 with dent at 20% load:

Post-impact fatigue behavior



Glare 5-2/1 with dent: Just impact behavior

Important Findings for Certification of GLARE (cont'd)

- **Post-Impact Fatigue**
 - Crack in impacted GLARE under fatigue loading only initiated and grew in the impacted, outside, inspectable Al layer
 - The stress state around the 3-D dent is complicated. A non-symmetrical stress state developed where high tensile stresses are experienced on the impacted side.
 - The propagation of cracks to the edge of the panel did not lead to catastrophic failure because the composite layer has sufficient residual strength to carry the fatigue load
 - The fatigue crack initiation life in the GLARE is shorter than the Al alloy. However, crack initiation life for GLARE is only a small fraction of the fatigue life whereas the crack initiation life is very close to fatigue life for Al alloy.

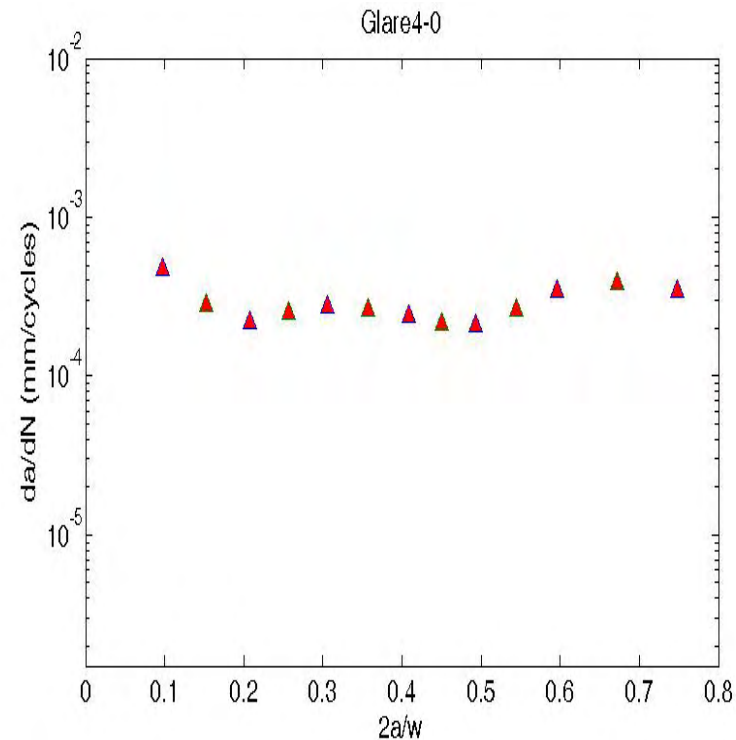
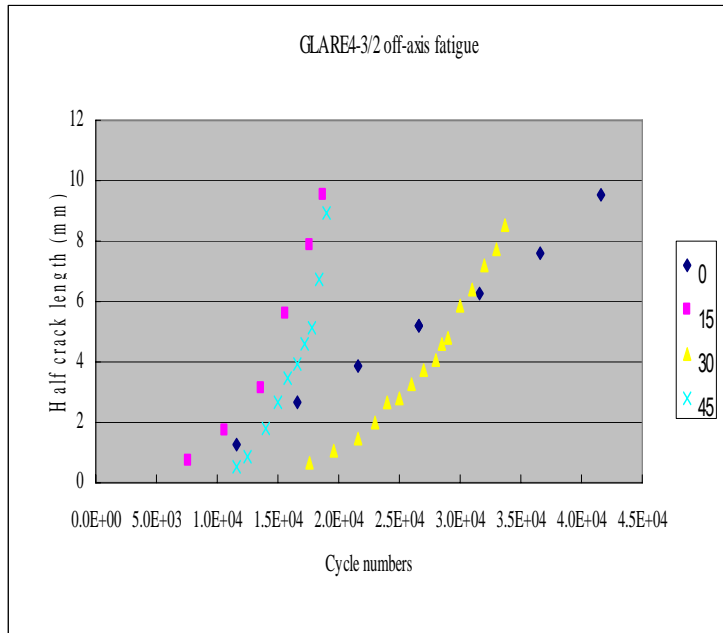
Important Findings for Certification of GLARE (cont'd)

- **Post-Impact Fatigue**
 - Crack in impacted GLARE under fatigue loading only initiated and grew in the impacted, outside, inspectable Al layer
 - The stress state around the 3-D dent is complicated. A non-symmetrical stress state developed where high tensile stresses are experienced on the impacted side.
 - The propagation of cracks to the edge of the panel did not lead to catastrophic failure because the composite layer has sufficient residual strength to carry the fatigue load
 - The fatigue crack initiation life in the GLARE is shorter than the Al alloy. However, crack initiation life for GLARE is only a small fraction of the fatigue life whereas the crack initiation life is very close to fatigue life for Al alloy.

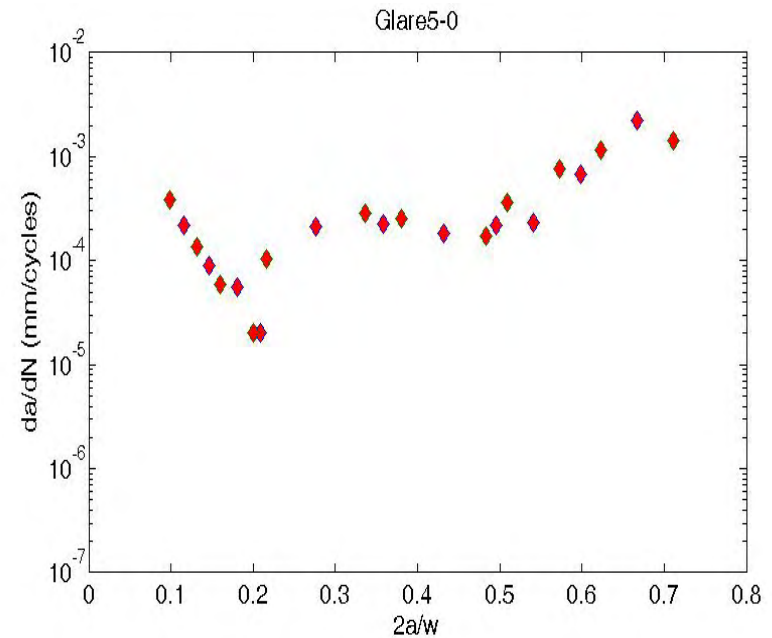
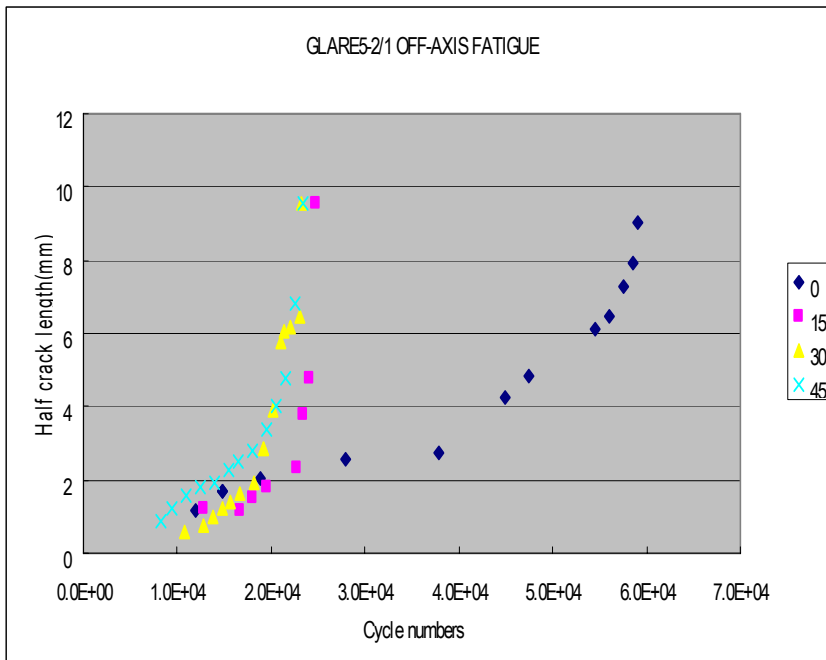
Experimental Set-up:

- Specimen with 0° , 15° , 30° , and 45° off-axis angles.
- Specimen geometries: 8×1 " with a center hole (0.25" in diameter)
- Constant amplitude fatigue testing with $R=0.1$ and $f=10$ Hz.
- For GLARE4-3/2, the applied loads are 40% and 30% of the notched strength.
- For GLARE5-2/1, the applied load is 40% of the notched strength.
- Crack length vs fatigue cycles were measured.
- The post-fatigue residual tensile strength was measured as well.

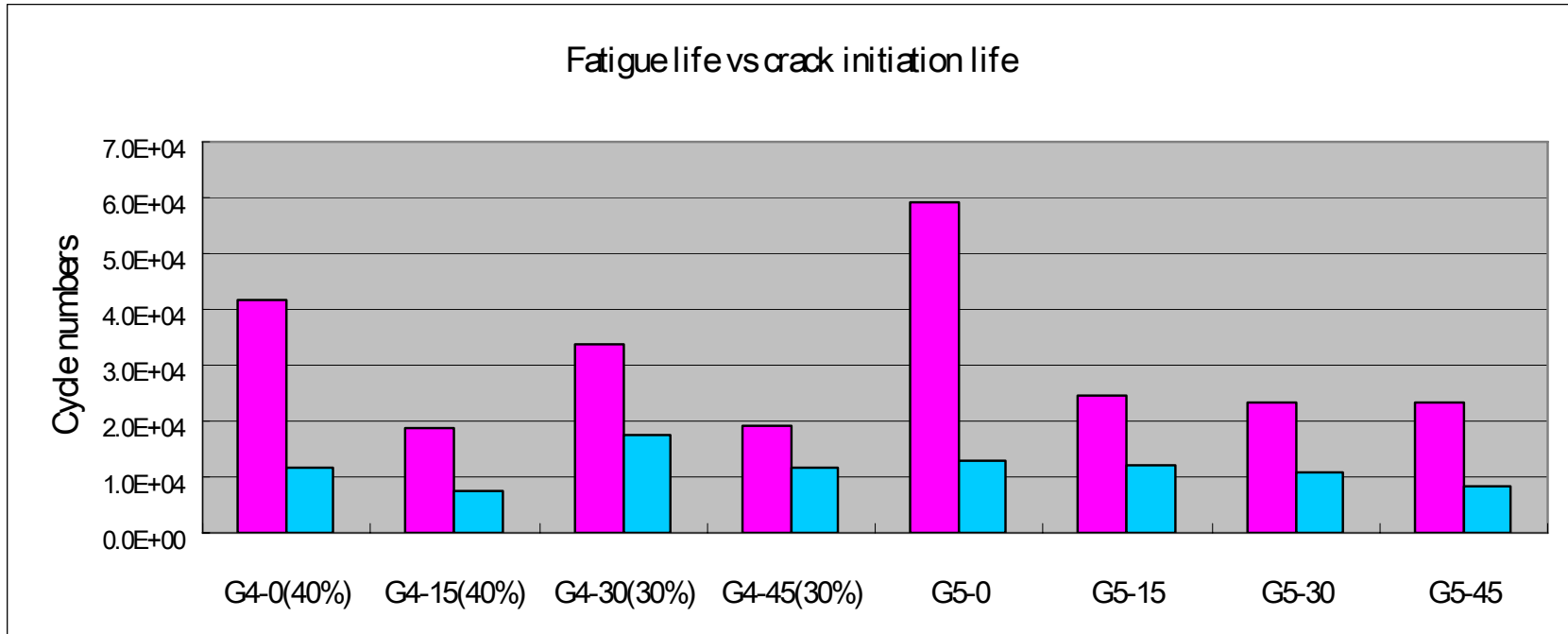
- As off-axis angles increase, the fatigue life decreases.
- For GLARE4-3/2 $\theta=0^\circ$ specimen, constant crack growth rates could be reached.



- As off-axis angles increase, the fatigue life decreases



- For GLARE4&5 off-axis specimens, the fatigue life decreases as off-axis angles increase.
- As the maximum applied load decreases, the fatigue life and crack initiation cycles increase for Glare4-3/2 off-axis specimens.



- Direction of crack propagation is not perpendicular to the fiber direction for the off-axis specimens.

Off axis $\theta=15^\circ$

Nucleation angle $\varphi=20^\circ$.

Off axis $\theta=30^\circ$

Nucleation angle $\varphi=14^\circ$.

Off axis $\theta=45^\circ$

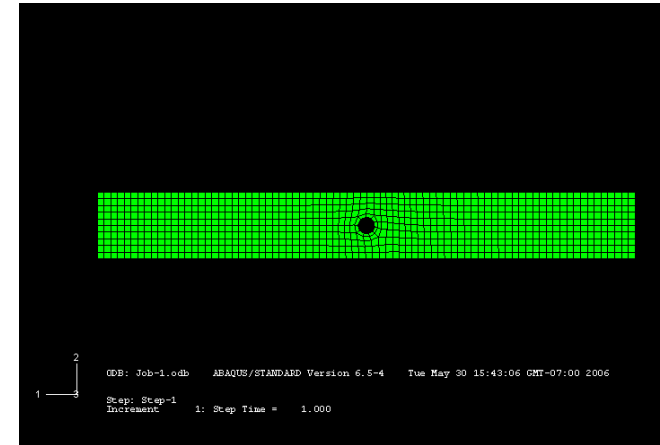
Nucleation angle $\varphi=8^\circ$.

Off axis $\theta=0^\circ$

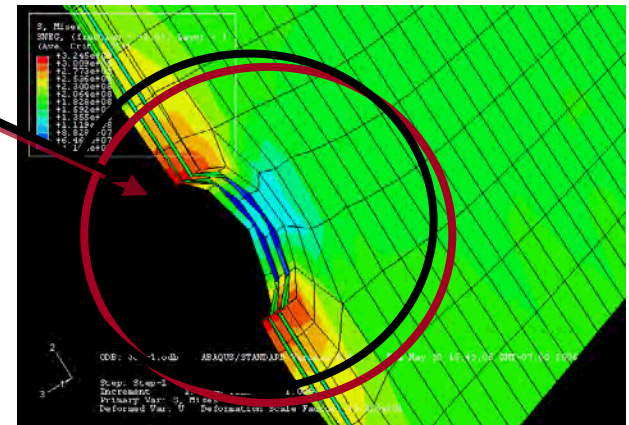
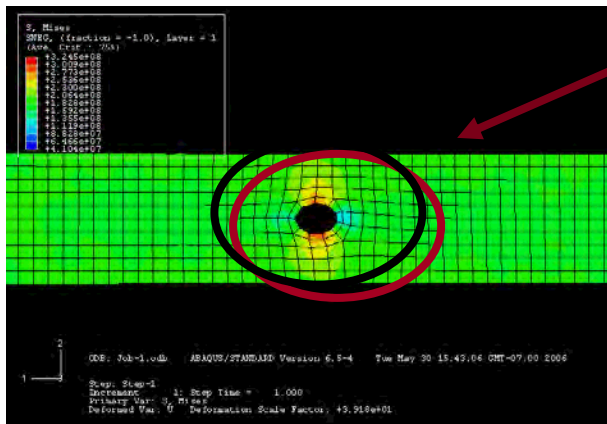
Nucleation angle $\varphi=0^\circ$.



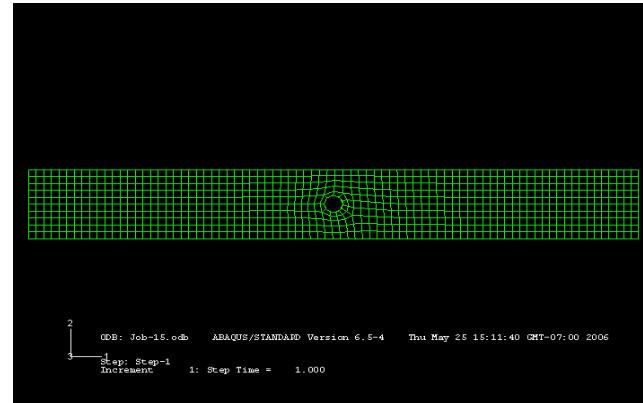
- GLARE4-3/2 -0 off-axis is modeled with ABAQUS.
- Before crack initiation, assuming there is no de-lamination presence.
- Boundary conditions: $R_x, R_y, R_z = 0$.
- Interface contact: Tie
- Applied load = 160Mpa



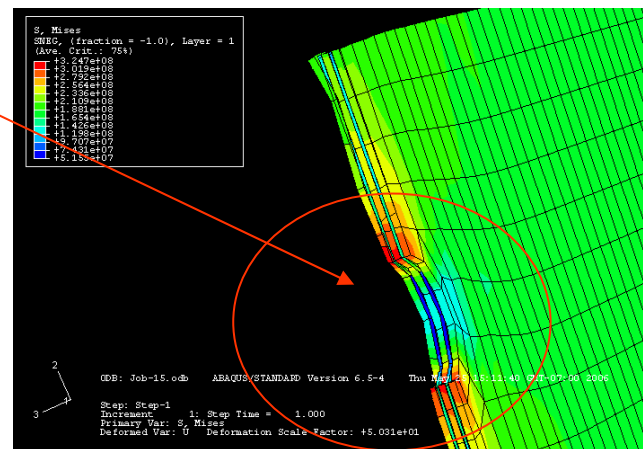
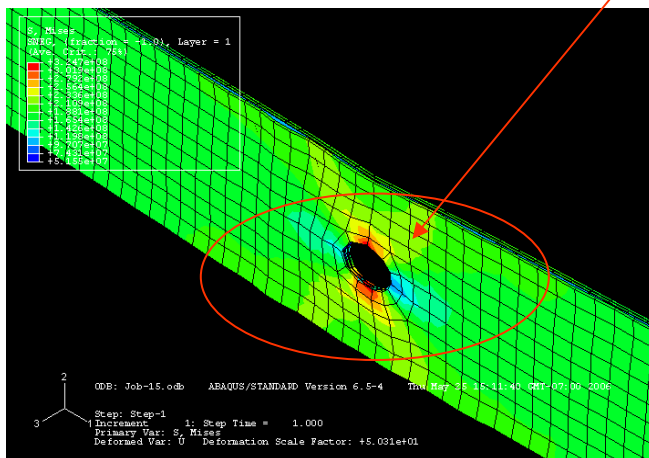
Maximum stress site.



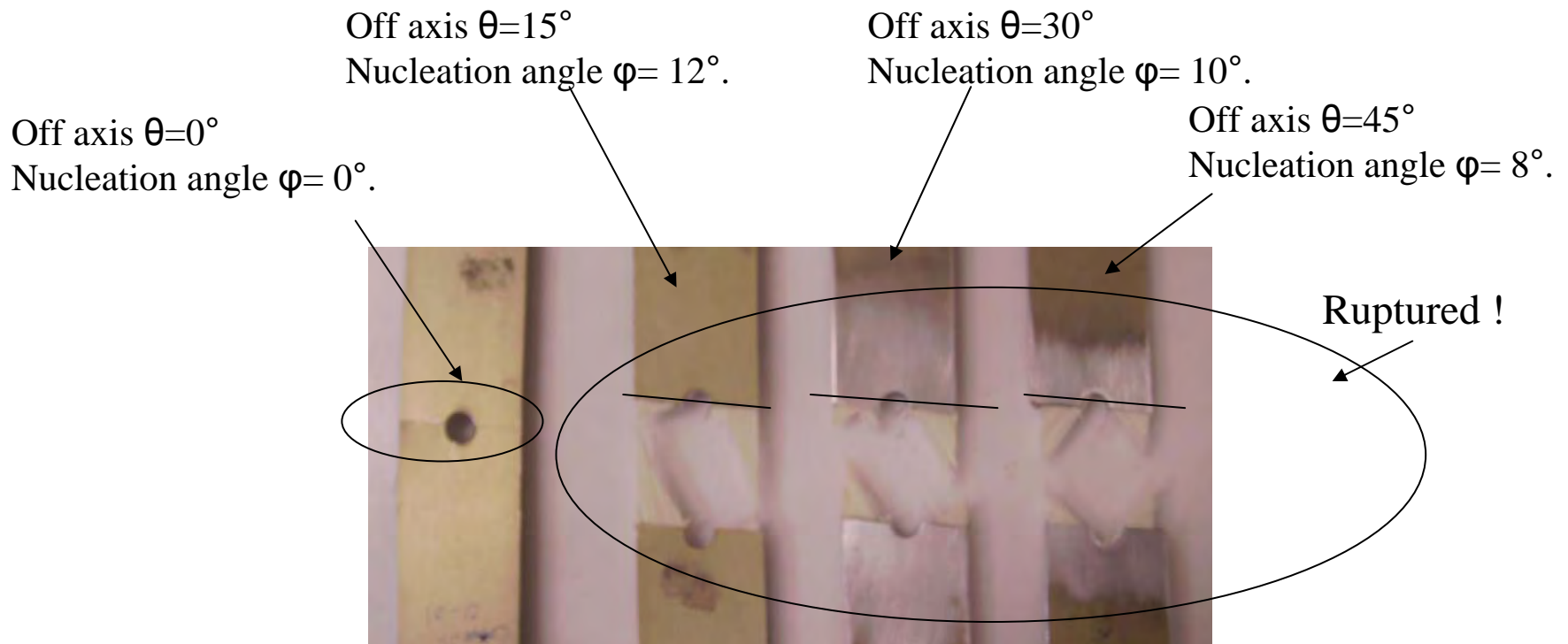
- GLARE4-3/2 -15 off-axis is modeled.
- Maximum stress intensity site oriented due to fiber orientations.
- Left: Undeformed shape.
- Bottom: Stress mapping on surface and cross-section.



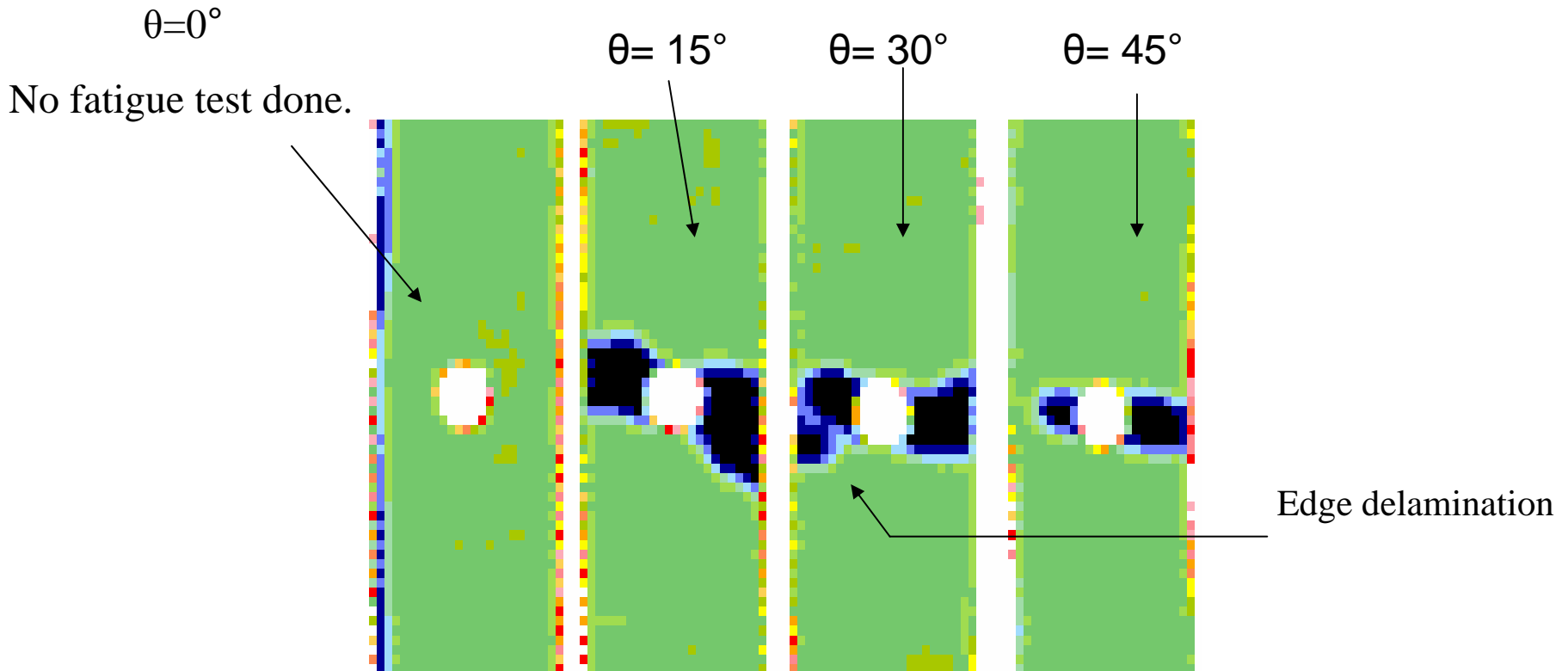
Oriented maximum stress site.



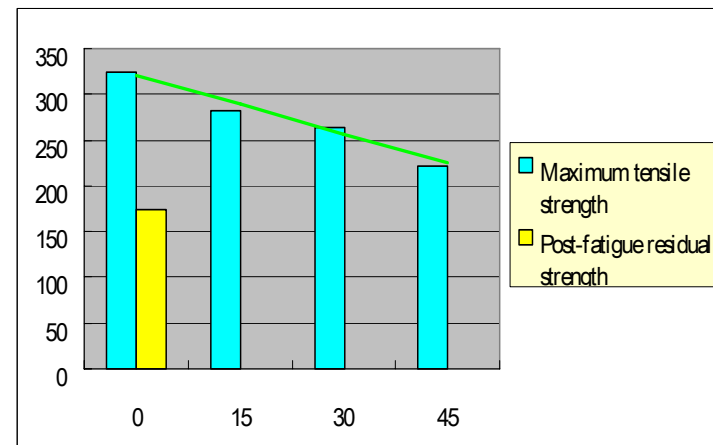
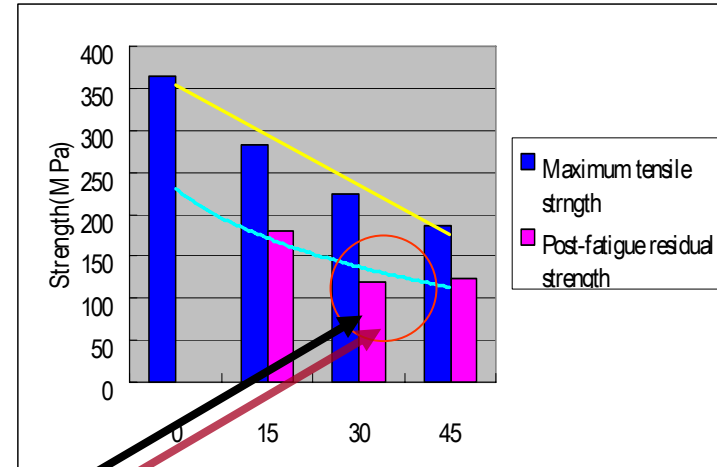
-Direction of crack propagation is not perpendicular to the fiber direction for the off-axis specimens.



-The delamination profiles are consistent with crack growth direction.



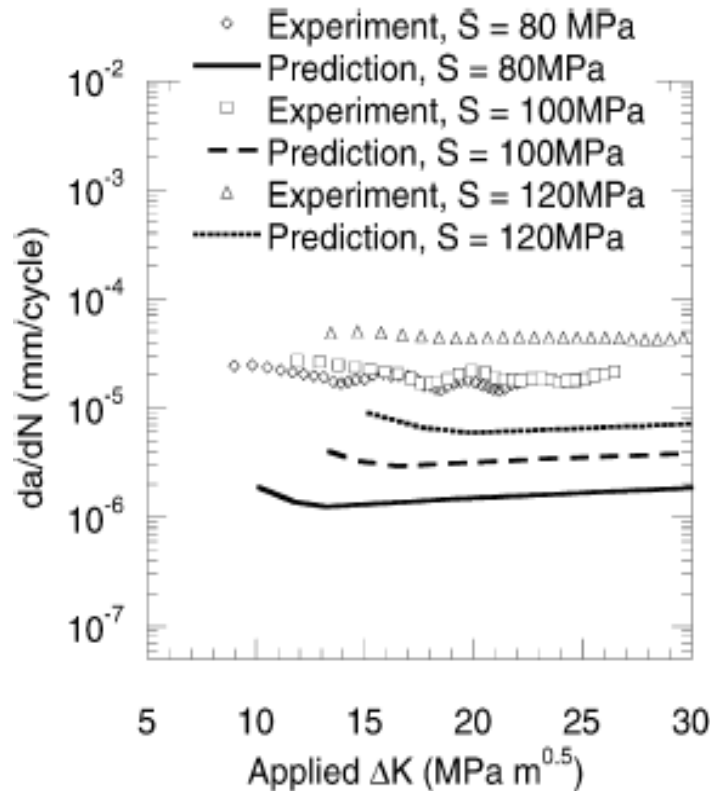
- The tensile strength decreased as off-axis angles increased for both GLARE4-3/2 and GLARE5-21 off-axis specimens.
- For GLARE4-3/2 specimens when the off-axis angles increase, the post-fatigue residual strength decreases.
- For GLARE5-2/1 off-axis specimens, they fractured during the fatigue tests except 0° off-axis coupon specimen.



Edge delamination

- Mechanism-based models
 - Calculating the effective stress intensity factor in the metal layer and strain energy release rate associated with de-lamination in the wake of the crack via a bridged crack model. The crack and de-lamination growth rates in the FML are then prediction using two power-law type empirical relationships.
- Mechanistic models
 - Using three-dimensional finite element analysis to obtain the model I stress intensity factor in the metal layer, a Paris-type power law is used to predict the crack growth rate in the FML.
- However, these models require a complicated analysis and there are discrepancies between the predictions and experimental results.

Fatigue Crack Growth Modeling for GLARE3-4/3 & 8/7



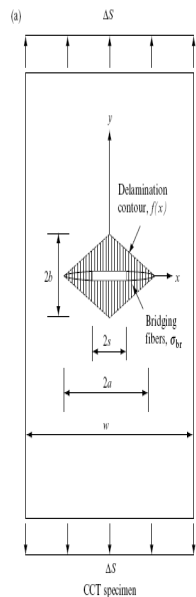
Predicted and experimental fatigue crack growth rates in GLARE3-8/7 type laminates under a maximum cyclic stress of 80,100, and 120 MPa using a generic power law

$$\frac{da}{dN} = 1.68 \times 10^{-11} (\Delta K_{eff})^{3.86}$$

D.J.Shim, R.C. Alderliesten, S.M. Spearing, D.A. Burianek, MIT
15 Jan 2003

- **A simple and more practical model for predicting crack growth**
- **Physical mechanism of steady crack growth: both crack growth and delamination depend directly on the bridging stress**
- **The effective stress intensity factor range actually experienced at the crack tip is also a constant as a result of constant crack growth**
- **It was assumed that with constant crack growth rate, the equivalent crack length is independent of cyclic loadings, the saw-cut size, the crack types and the specimen width.**
- **The equivalent crack length is only affected by the lay-up of the laminates.**

- Walker's type equation applicable to GLARE(Constituent metal is AL-2024-T3)
- Crack growth constants of the constituent metal in GLARE :C, m, &n determined experimentally by curve fitting..



$$\frac{da}{dN} = C[(1 - R_c)^{m-1} \Delta K_{eff}]^n$$

$$\Delta K_{eff} = \frac{\sqrt{l_0}}{\sqrt{(a-s) + l_0/F_0^2}} \Delta S_{eff} \sqrt{\pi a}$$

If $S_{max} \leq S_{op}$, there is no crack growth,
if $S_{min} < S_{op} < S_{max}$

$$\Delta S_{eff} = S_{max} - S_{op} \quad \text{and} \quad R_c = 0$$

if $S_{op} \leq S_{min}$,

$$\Delta S_{eff} = S_{max} - S_{min} \quad \text{and} \quad R = \frac{S_{min} - S_{op}}{S_{max} - S_{op}}$$

Crack opening stress obtained from Dugdale model:

$$S_{op} = -\frac{2}{\pi} \arccos \left[\frac{\sin(\pi s/W)}{\sin(\pi a/w)} \right] \frac{E_{lk}}{E_{Al}} \sigma_{r,Al}$$

$\sigma_{r,Al} = \text{residual_stress}$

$$F_o = \sqrt{\sec(\pi s/w)}$$

Schematic of center-crack tension specimen

Ya-Jun Guo*, Xue-Ren Wu, Composites Science And Technology 12 Feb 1999

Calculation of Equivalent Crack Length

- Equivalent crack length was determined experimentally by using Walker's type equation.

$l_o = \text{equivalent_crack_length}$

$$l_o = \frac{\gamma^2}{\frac{1}{F^2} - \frac{\gamma^2}{F_o^2}} \cdot (a - s)$$

$$\gamma = \Delta K_{\text{eff}} / \Delta K$$

$$\Delta K = \sqrt{\sec(\pi a / w)} \cdot (S_{\text{max}} - S_{\text{min}}) \sqrt{\pi a}$$

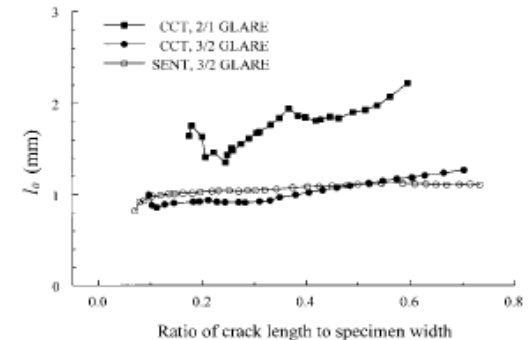
$$\Delta K_{\text{eff}} = \frac{n \sqrt{da/dN}}{n \sqrt{C_1 (1 - R_c)^{m-1}}}$$

$$F = \sqrt{\sec(\pi a / w)}$$

$$R_c = \frac{S_{\text{min}} - S_{\text{op}}}{S_{\text{max}} - S_{\text{op}}}$$

$$F_o = \sqrt{\sec(\pi s / w)}$$

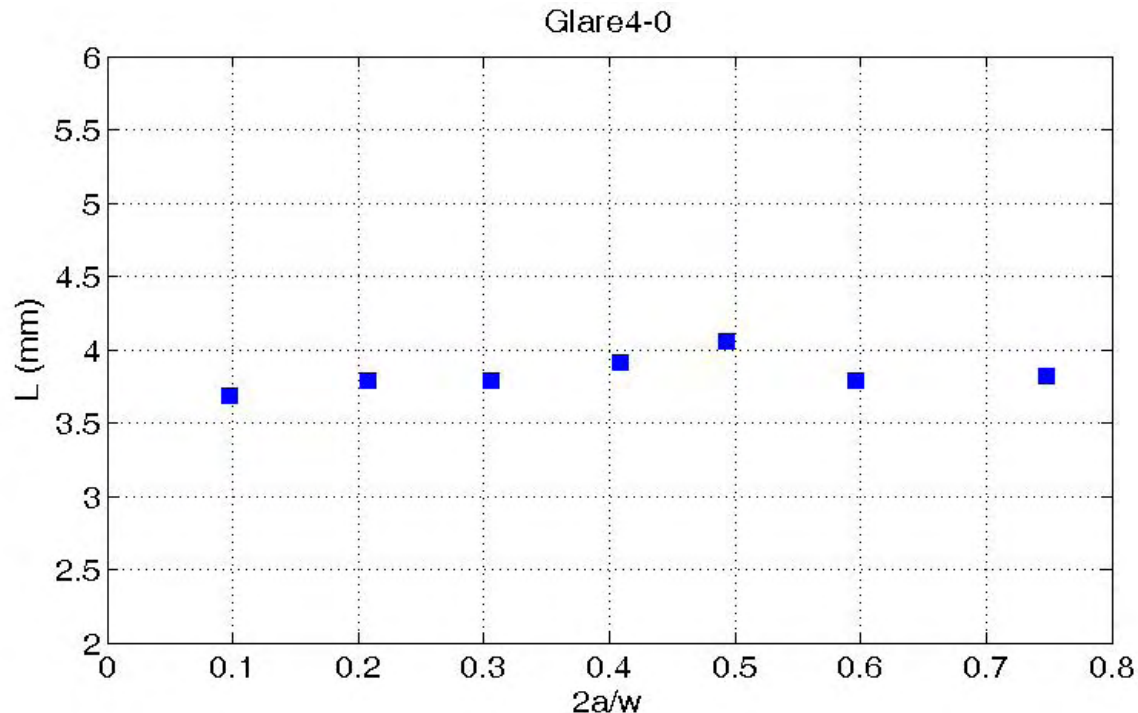
Equivalent crack length against 2a/w



Ya-Jun Guo*, Xue-Ren Wu, Composites Science And Technology 12 Feb 1999

Equivalent crack length GLARE4-3/2

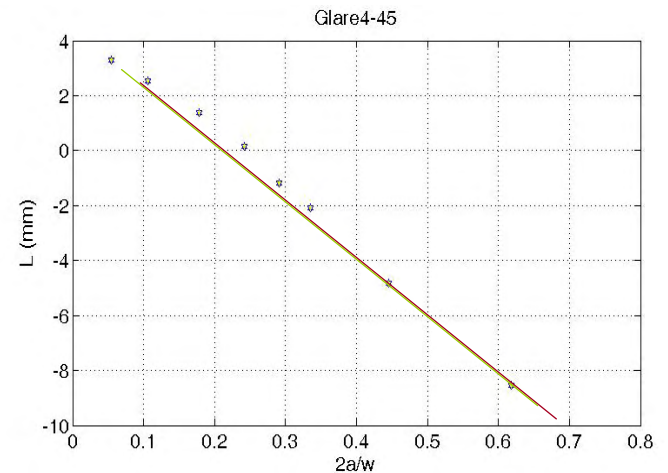
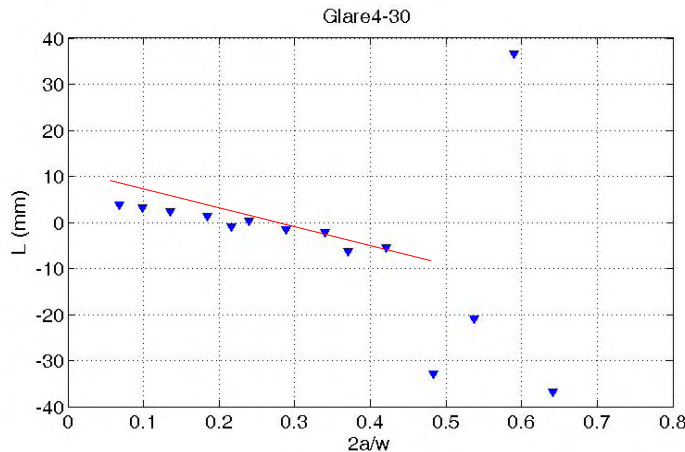
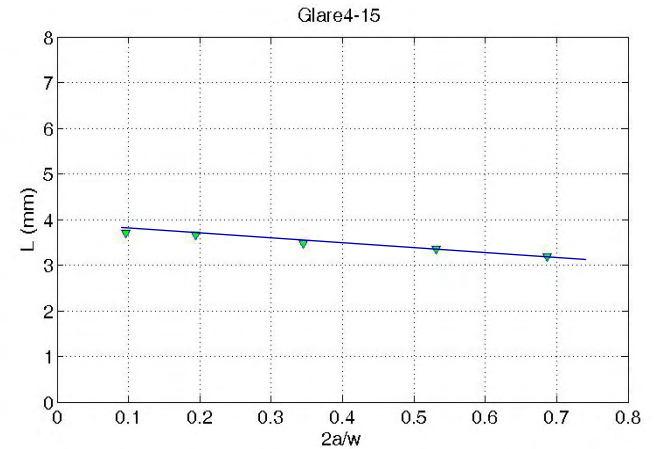
- For Glare4- $\theta=0^\circ$, $L= 3.75$ mm
- The equivalent crack length was assumed to be constant for constant growth rate.



Equivalent crack length for off-axis GLARE4-3/2

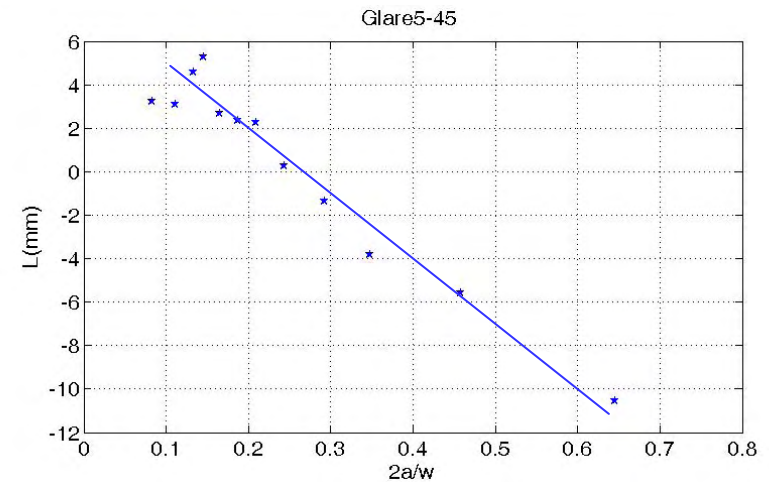
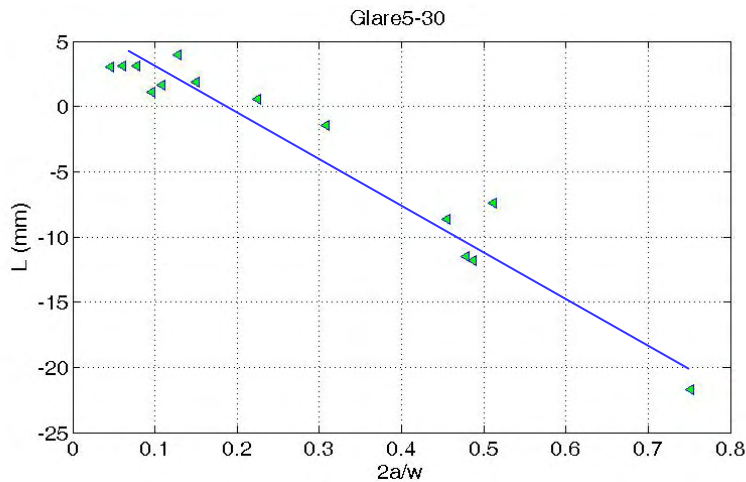
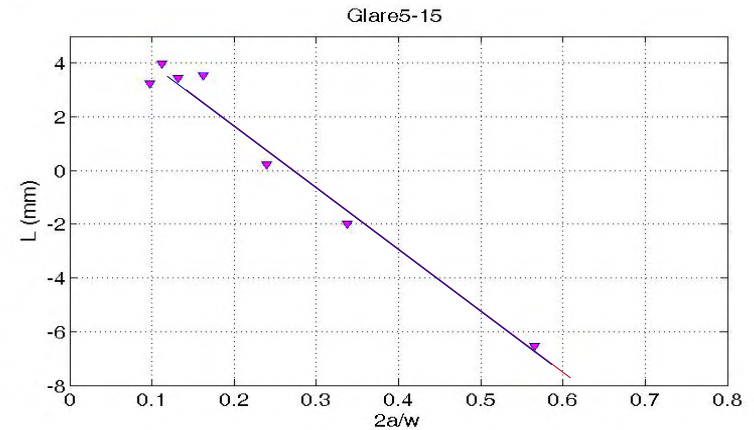


Model failed for the off-axis fiber metal laminates and needed to be modified.



Equivalent crack length for off-axis GLARE5-2/1

Model failed for the off-axis fiber metal laminates and needed to be modified.



Off-axis phenomenological model GLARE4&5

- Based on observation of L v.s. $2a/w$, we propose

$$L = f\left(l, \frac{2a}{w}\right)$$

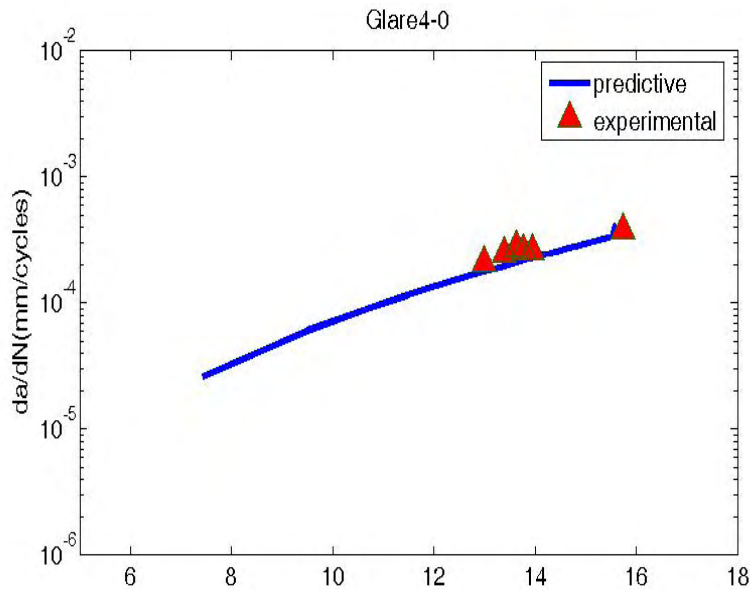
$$L_i = l_i + m_i\left(\frac{2a_i}{w_i}\right) + \Delta$$

Where a is the crack length, w is the width, m is the slope and l is initial characteristic crack length. Ignore the high order terms.

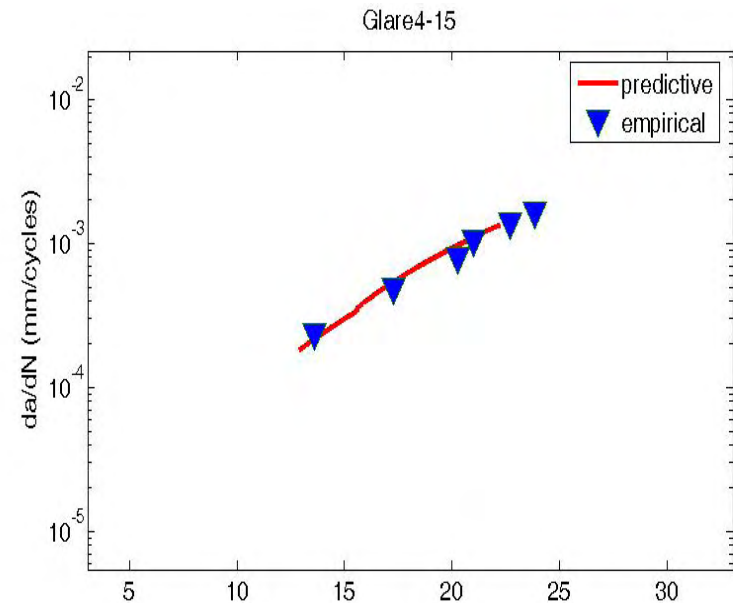
And, for constant growth rate, $m = 0$.

Effective Stress Intensity Range GLARE4

- For GLARE4-2/1 $\theta=0^\circ$ off-axis, a constant equivalent crack length is applied.
- Good agreement is achieved between tested results and off-axis model.

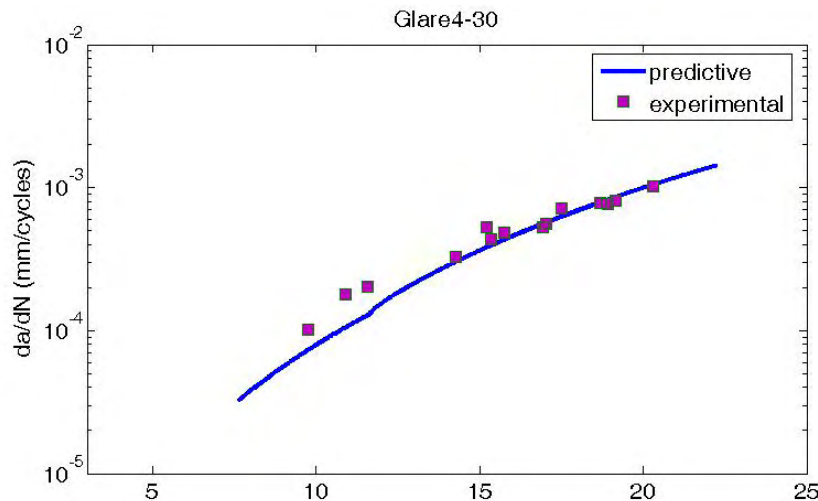


$\Delta K_{eff} (MPa \cdot m^{1/2})$

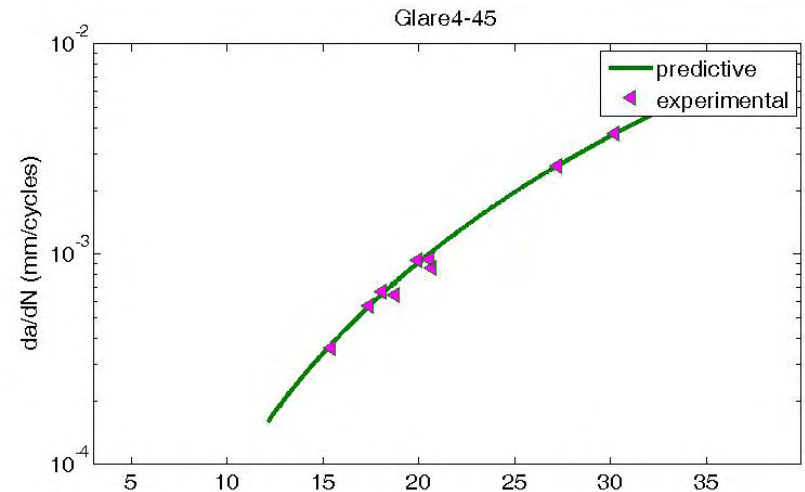


$\Delta K_{eff} (MPa \cdot m^{1/2})$

- For off-axis specimens, the modified equivalent crack length is applied.
- Good agreement could be achieved between tested results and off-axis fatigue model.



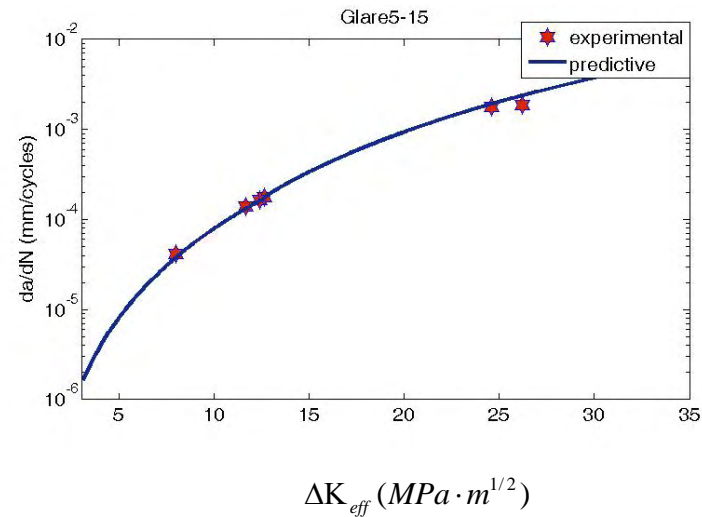
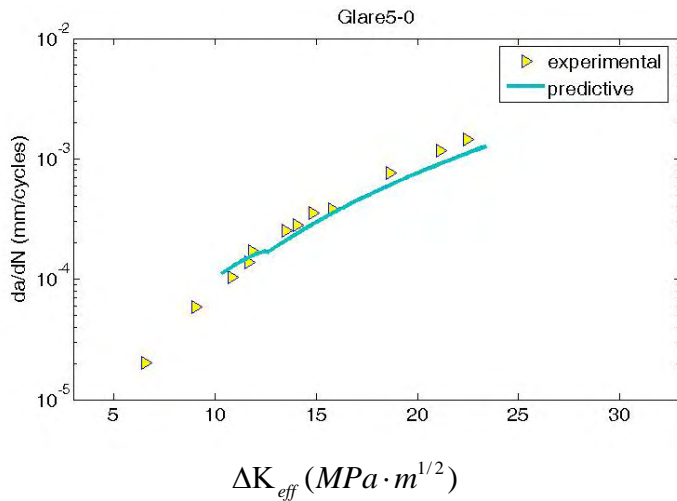
$\Delta K_{eff} (MPa \cdot m^{1/2})$



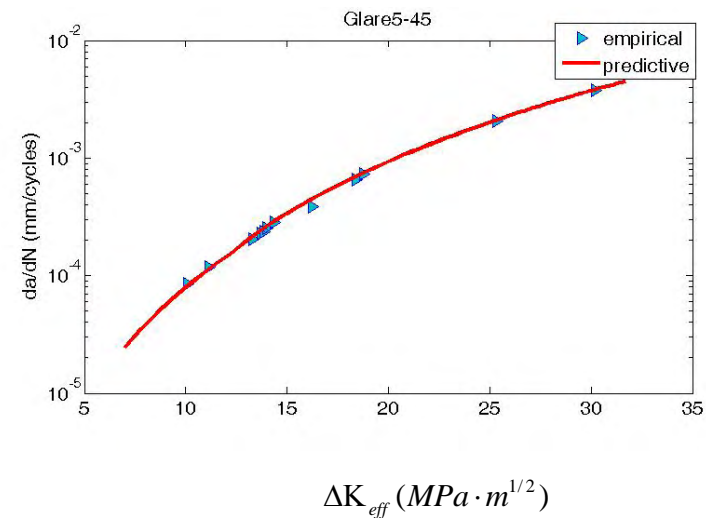
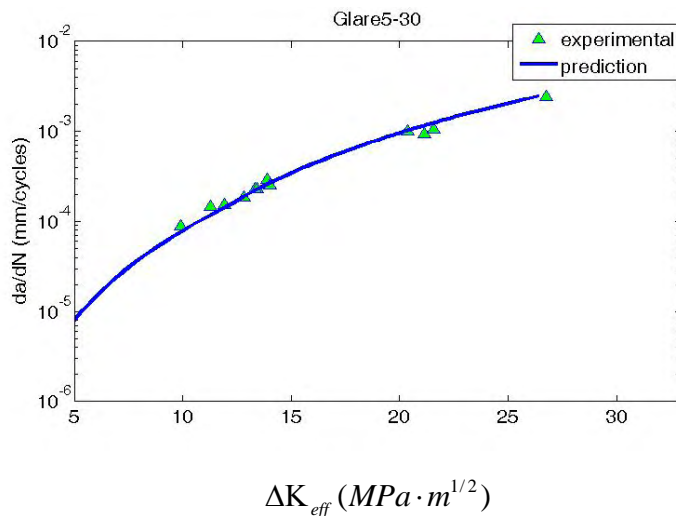
$\Delta K_{eff} (MPa \cdot m^{1/2})$

Fatigue Crack Growth Prediction for GLARE5

- For GLARE5-2/1 $\theta=0^\circ$ and 15° off-axis, the crack growth rate could be predicted by applying the modified off-axis fatigue model.



- For GLARE5-2/1 $\emptyset=30^\circ$ and 45° off-axis specimens, good agreement was achieved with the tested data based on the off-axis phenomenological fatigue model .



Important Findings for Certification of GLARE (cont'd)

- **Constant Amplitude Fatigue**
 - Fatigue crack initiated mainly in the Al layer in GLARE. Al layer carried more load than the composite layers due to their high stiffness
 - Crack growth and delamination form a balanced mechanisms in which both process are continuously influencing each other during fatigue life
 - Fatigue crack growth rate is sensitive to fiber orientations. Crack growth rates increase as the off-axis angle increases due to less effective bridging effect and larger delamination zone
 - A simple phenomenological model could be used to predict the crack growth behavior in various GLARE laminates and different loading directions.

Information System for GLARE

- Database for GLARE laminates: collect and compile experimental data from published literatures.
- The developed information system for the GLARE provides analysis over multiple sets of data collected under different experimental studies
- It allows for the comparison of different GLARE with various geometry and loading condition

Data Entry

Data Enterer

Date Record:

Data Enterer Last Name: Data Enterer First Name:

Unit System:

References

Publication Name: Publication Year:

Reference Title:

Funding Agency:

First Author Last Name:

First Author First Name:

Second Author Last Name:

Second Author First Name:

Compression Testing	Other Impact Info	Data Source
Manufacturing Info	Environmental Conditions	NDE Methodology

Paper Number: Test Number: Next Page >

- The first configuration is to compile the information from literatures related to GLARE
- It consists of the following tables: authors, data enterer, and references, notes, data source

Data Entry

Material System | Material Property(Undamaged) | Configuration | Structure

Impact Parameters | Damage Characteristics | Fatigue Parameters | Bearing Parameters

Impact Parameters

Impact Type: Static
 Impact Fixture: OTHER
 Length: 100
 Width: 100
 BCs: C-C-C-C
 Impactor Mass:
 Impactor Radius: 7.5
 Total Thickness: 0.83

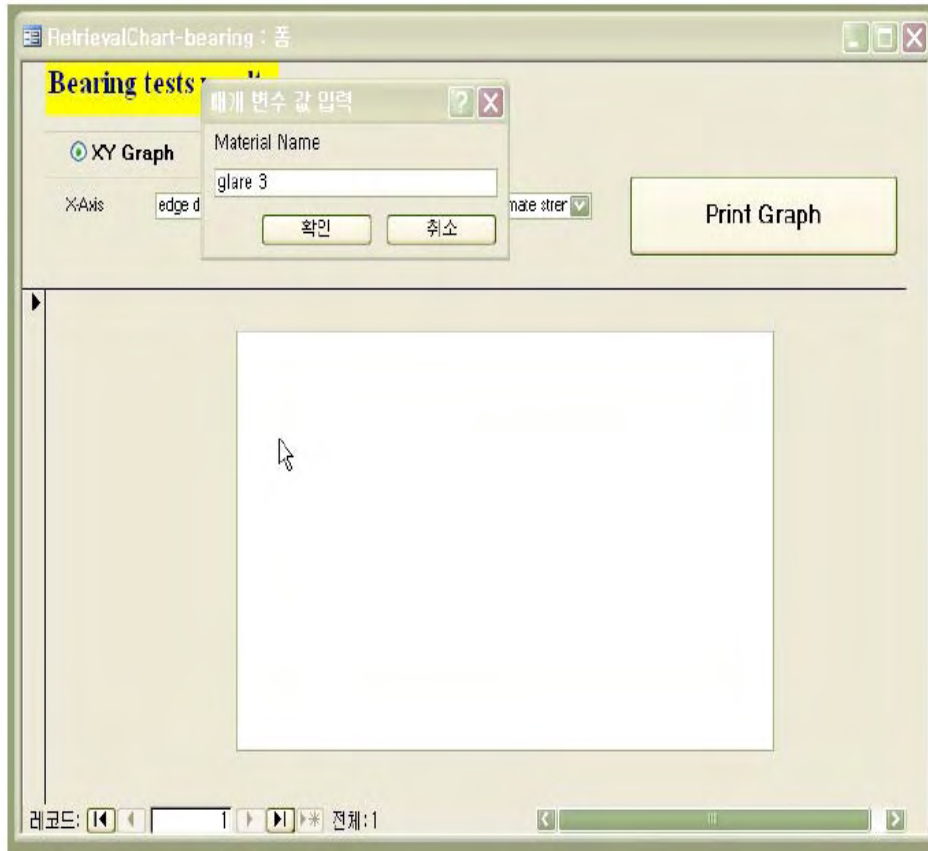
Areal Density: 2.2
 Impactor Velocity: Static
 Impact Damage: Penetration
 First Failure Energy: 15.1
 Through Crack Energy: 15.1
 Impact Location: center
 Impact Force: 0

레코드: 1 전체: 24

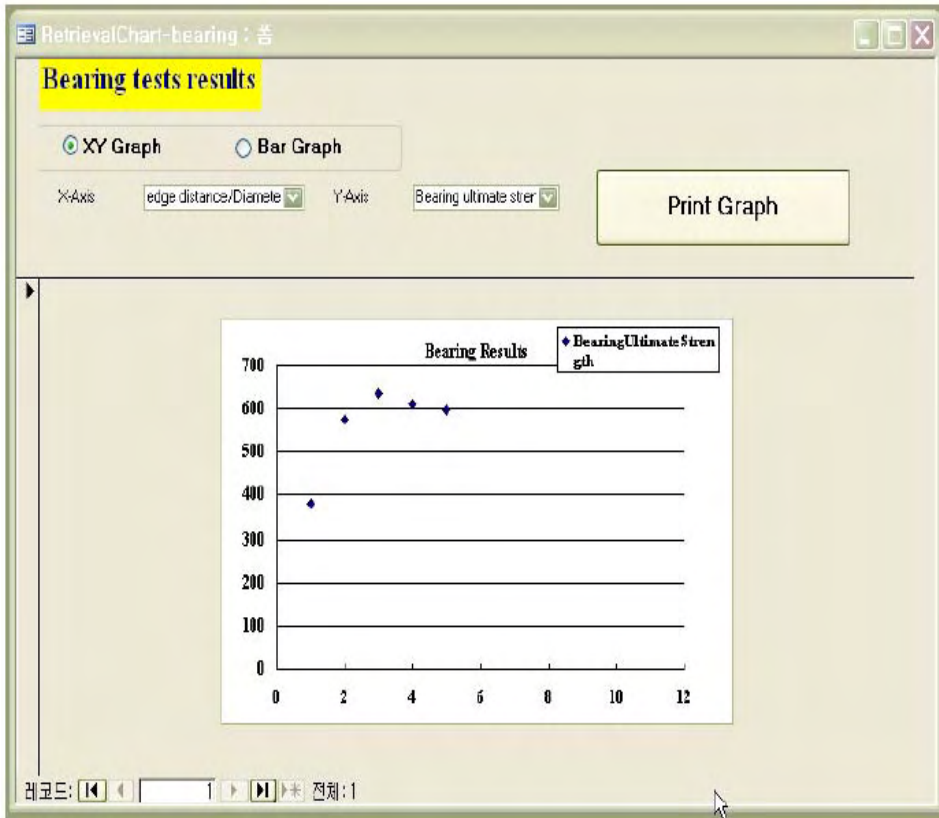
New Test | Delete Test | < | < | > | >

Paper Number: 1 | Test Number: 1 | < Previous Page | 2

- The second configuration is to organize the information for GLARE including mechanical properties, experimental parameters etc



- Data retrieval system is based on query system
- A query lets you ask all kinds of questions about the information of GLARE that is stored in your database.
- As seen in figure, you can choose the material name, layer number, load type by using window box



- Example: variation of pin-type bearing ultimate strength of GLARE 2-2/1
- By choosing x-axis (e/D) and y-axis (bearing ultimate strength), the data based on query table were able to plot with chosen option as seen in figure

- Fatigue cracking in the Al layers appears to be inevitable
- Can we live with the crack? (probably not)
- How do we contain the crack?
- How do we prevent the cracking?

- Benefit to Aviation
 - Development of analytical models validated by experiment and the information system are critical to design optimization and to support the certification.
- Future needs
 - Variable amplitude fatigue behavior
 - Constant and variable amplitude fatigue of mechanically fastened joints
 - Lightning strike resistance